The Sensitivity of Two-Dimensional Simulations of Tropical Squall Lines to Environmental Profiles

MELVILLE E. NICHOLLS, RICHARD H. JOHNSON AND WILLIAM R. COTTON

Department of Atmospheric Science, Colorado State University, Fort Collins, Colorado

(Manuscript received 15 December 1987, in final form 16 June 1988)

ABSTRACT

Two-dimensional experiments are carried out to determine the effect of various wind and thermodynamic structures on squall line characteristics. Two ideas concerning the effect of shear are found useful in explaining many of the outcomes of the numerical experiments. First, in two dimensions, shear in the absence of vorticity sources and sinks is detrimental to convection (Kuo, Asai). Second, there is a specific value of low-level shear interacting with a cold pool which produces deep uplift and hence strong forcing of convection (Rotunno et al.). Results suggest that moist midlevel air tends to be favorable for squall lines. Increasing the total buoyancy or altering the distribution of buoyancy with height, such that it is increased at low levels, produces stronger systems with updrafts more tilted from the vertical.

The formula by von Kármán for the speed of a gravity current gives qualitative agreement with the speed of most of the simulated systems. However, at least two additional factors need to be considered to accurately determine propagation speed. First, the wind speed ahead of the system can be modified from environmental values. Second, the propagation speed depends on the surface pressure jump across the gust front and this is not always accurately determined by the temperature anomaly in the shallow cold pool. A diagnosis of the contributions to the surface pressure jump shows that the warming external to the cold pool and waterloading can be significant. It is found that for vertically oriented or downshear tilted updrafts, the positive contribution to the pressure jump due to waterloading can sometimes exceed the negative contribution due to warming. This results in the system moving faster than predicted by the gravity current model whereas, for an upshear tilted updraft, the effect of warming can outweigh waterloading, causing the system to move slower.

An examination of the vorticity balance that occurs for a case having a vertically oriented updraft suggests that it cannot be regarded as purely one between the environmental shear and the cold pool.

1. Introduction

A previous study (Nicholls 1987, hereafter referred to as N87) demonstrated the ability of a two-dimensional cloud model to successfully simulate the major observed features of the squall line that occurred on 12 September of GATE (The Global Atmospheric Research Programs Atlantic Tropical Experiment). In this paper the aim is to further our understanding of tropical squall lines by comparing and contrasting the results of experiments in which the environmental wind and thermodynamic structure are varied.

Earlier two-dimensional numerical modeling studies of squall lines have investigated the effect of the environmental wind profile (Hane 1973; Thorpe et al. 1982; Dudhia et al. 1987). Hane (1973) used an environment typical of that found for squall lines that occur in the southeastern United States in summer. This environment was characterized by strong vertical shear and dryness of the air in midtropospheric levels. Experiments demonstrated the importance of strong wind shear in producing a long lasting system. It was found that the updraft had an upshear tilt at lower levels and a downshear tilt at upper levels. The downshear tilt at upper levels was more prominent later in the simulation, leading to the detrimental effect of rain falling into the updraft region. Although a jet profile (a feature typical of tropical squall lines) was not included in these experiments, a case with strong shear below 3 km with hardly any shear above produced a more persistent upshear tilt than for the other cases which had unidirectional[1] shear. Thorpe et al. (1982) performed numerical experiments which included both unidirectional shear and jet-profiles. The case with strong low-level shear but no upper-level shear produced the most intense system. Simulations with unidirectional shear were found to be unsteady. Jet profiles

Corresponding author address: Dr. Melville E. Nicholls, Dept. of Atmospheric Science, Colorado State University, Fort Collins, CO 80523.

[1] Here the term "unidirectional shear" refers to a wind shear that does not change sign with height. Sometimes it is used to describe hodographs for which the wind profile lies in a straight line, with height values lying anywhere along that line.

led to less vigorous but nevertheless quasi-steady circulations. Dudhia et al. (1987) simulated a tropical squall line that occurred over West Africa. It existed in an environment having a low-level easterly jet. The simulated system was multicellular, with cells periodically being generated and traveling downstream relative to the gust front. Modifying the wind profile by significantly reducing the magnitude of the shear above the easterly jet was found to lead to a very steady unicell type of circulation. In this case the updraft was more upright. A surprising aspect of the simulation was the absence of a significant cold pool, the circulation appearing to exhibit wave-like behavior. Low-level inflow air flowed through the cold pool so there was no stagnation point at the surface.

Heretofore, all squall lines which have been the subject of detailed observational analyses have possessed a cold pool, which is fed by cool convective scale downdrafts. Strong convergence at the gust front head helps to initiate new convective cells. Clearly, the propagation speed of the system as a whole is likely to be linked to the speed of the gust front (Moncrieff and Miller 1976). Just how the properties of the cold pool are related to the environmental structure the squall lines forms in is of considerable interest.

A recent study by Rotunno et al. (1988) considers the optimum condition for producing uplift at the gust front. According to this theory the optimum condition occurs when the import of vorticity associated with low-level environmental shear balances the circulation induced by the cold thunderstorm outflow. When this condition is satisfied the updraft is a vertically oriented jet. Numerical experiments show that this leads to deeper, less inhibited lifting. Hence, in the presence of a cold pool, low-level shear can be beneficial to convection. In the absence of a cold pool a number of investigators (Kuo 1963; Asai 1964; and others) have shown that shear inhibits convection in two dimensions. Asai (1964) found that rising thermals tilt downshear and a countergradient momentum transport occurs which causes convective potential energy to be transformed into the horizontal kinetic energy of the mean flow. Furthermore, in the presence of shear the axis of the updraft and temperature in a rising thermal do not coincide as they do in the absence of shear. This reduces the buoyant generation of convective energy. Another factor, suggested by Lilly (1985), is that as updrafts tilt downshear, both convective and shearing instabilities become possible. The eventual break up of the original updraft into a series of convective and shearing instabilities would produce the detrimental effect of increased mixing with the environment. It is of considerable interest to ascertain whether the results of this study are consistent with these ideas.

There is little known about the effects various thermodynamic structures have on squall line characteristics. A commonly held view is that dry midlevel air is more favorable for squall lines than moist midlevel air. One reason is that the convective instability is larger (θ_e has a more pronounced minimum). Furthermore, drier midlevel air should favor evaporative cooling and downdrafts, thus aiding the formation of a cold pool. However, the entrainment of drier air at midlevels might have a detrimental effect on updrafts. There has not yet been any modeling studies of squall lines to determine the sensitivity to midlevel moisture. Szoke and Zipser (1986) conjecture that the stronger updraft strengths found in cumulonimbi at midlatitudes over land compared with those in the GATE region, for similar net CAPE's, are due to a different distribution of buoyancy with height. They suggest that having the buoyancy concentrated at low levels produces stronger updrafts. Whether this carries over to squall line updrafts is one of the questions we attempt to answer in this study. Furthermore, there is little known quantitatively of how the amount of buoyant energy effects squall line properties.

This study attempts to provide a more complete picture of the importance of environmental structure on the propagation speed, intensity, and structure of tropical squall lines. The numerical model is a powerful tool in this respect, since controlled experiments can be carried out where one parameter is changed at a time with everything else remaining the same. Although there have been some investigations of the effects of different wind profiles on tropical squall line characteristics, there has not been a comprehensive study. In addition to varying the wind shear above the low-level jet, experiments are carried out in which the strength and height of the jet are altered. Furthermore, simulations involving changes to the thermodynamic structure are run, to determine how changing the magnitude of buoyant energy, the distribution of buoyant energy with height, and the amount of midlevel moisture effects squall lines.

The domain size used in this study is considerably larger than used in previous investigations, and the resolution finer. Moreover, the microphysical parameterizations include the ice phase, unlike earlier studies. The release of latent heat of fusion was shown in N87 to lead to stronger updrafts at upper levels in tropical squall lines.

In section 3 the various environmental structures used for the experiments are described. In section 4a the control case is discussed. In section 4b a general comparison of the results is presented, whereas in section 4c some individual simulations are discussed in more detail. Some general properties of the systems are described in section 4d, with particular emphasis placed on the factors influencing propagation speed. Finally, the vorticity balance that exists for a unicell system having a vertical updraft, is examined.

2. Description of the cloud model

The reader is referred to N87 for a more detailed description of the model used in this study. The cloud

model used is the Colorado State University Atmospheric Modeling System (RAMS). The model contains a full set of nonhydrostatic compressible dynamic equations, a thermodynamic equation, and a set of microphysics equations for water- and ice-phase clouds and precipitation. The horizontal grid spacing is 500 m and the vertical resolution is variable, corresponding to pressure increments of approximately 35 mb up to a height of 10 km, above which a constant spacing of 0.9 km is used. Domain size for all experiments is 300 km in the horizontal and 23 km in the vertical. The upper and lower boundaries are rigid walls. A weak dissipative layer approximately 8 km deep is included at the top of the domain to reduce reflection from the upper boundary. The lateral boundaries incorporate a mesoscale compensation region (MCR—see Tripoli and Cotton 1982). The MCR is included to provide a large-scale mass balance adjustment due to circulation trends generated within the interior model domain. Lateral boundaries of the fine-mesh domain additionally incorporate the Klemp–Lilly (1978) radiation boundary condition to allow propagation of gravity waves through the fine mesh/MCR walls. At the lower boundary frictional effects and surface fluxes are neglected.

3. Description of experiments

The wind and thermodynamic structure for the 12 September squall line is described in N87. Beneath 800 mb the air is moist, whereas at midlevels it is fairly dry. The sounding is conditionally unstable, with a lifted index of −5°C at 500 mb. The wind profile has both upper- and lower-level easterly jets. The magnitude of the shear is large both beneath and above the low-level easterly jet. The experiments which involve modification of this environment are listed in Table 1. The first group of experiments (group A) involves changes to the wind profile only and are portrayed in Fig. 1. In experiments A1, A2, and A3 (Fig. 1a), the magnitude of the low-level jet is varied. Values of jet maximum range from zero (no jet at all), to 15 m s^{-1}. Experiments A4 and A5 (Fig. 1b), have low-level jets of similar strengths, but at different heights. In experiments A6, A7, A8 and A9, the winds above the low-level easterly jet between approximately 300 and 600 mb, are varied as shown in Fig. 1c. In experiment A10, the jet speed is increased as in A1, and the shear aloft significantly reduced as in A7. In order to keep the systems within the domain a constant wind speed of 9 m s^{-1} is added to these wind profiles. The experiments listed in Table 1 are assigned a specific description. It should be noted that A8, the case of unidirectional shear, has weak shear aloft as does A7, but of opposite sign. Furthermore, A9 which is described as having stronger shear aloft, refers to the winds immediately above the low-level jet.

TABLE 1. List of experiments.

Group	Group no.	Experiment
(A) Changes to wind structure	A1	Stronger jet
	A2	Weaker jet
	A3	No jet
	A4	Higher jet
	A5	Lower jet
	A6	Reduced shear aloft
	A7	Weak shear aloft
	A8	Unidirectional shear aloft
	A9	Stronger shear aloft
	A10	Stronger jet and weak shear aloft
(B) Changes to thermodynamic structure	B1	Increased midlevel moisture
	B2	Decreased midlevel moisture
	B3	Increased buoyancy
	B4	Increased lowlevel buoyancy
(C) Changes to both wind and thermodynamic structure	C1	Increased buoyancy and weak shear aloft
	C2	Increased buoyancy and unidirectional shear
	C3	Increased buoyancy, stronger jet and weak shear aloft
	C4	Increased buoyancy and stronger jet
	C5	Increased buoyancy and weaker jet
	C6	Increased low-level buoyancy, stronger jet and weak shear aloft
	C7	Weak shear aloft and increased moisture

The second group of experiments (group B) involves changes to the thermodynamic structure only and are portrayed in Fig. 2. In experiment B1 the midlevel moisture is increased, whereas in B2 it is decreased (Fig. 2a). In experiment B3, the buoyant energy is increased by lowering the temperature above the boundary layer as shown in Fig. 2b. The value of CAPE is approximately 16% more than for the control case. In experiment B4, CAPE is approximately the same as for the control case, but buoyancy is concentrated at lower levels, as shown in Fig. 2c. This was effected by changing the temperature profile, decreasing it at low levels and increasing it at higher. Note that in this case the equilibrium level of an unmixed parcel risen from the surface is only 10.5 km, compared to 12.5 km for the original sounding.

The third group of experiments (group C) involves changes to both wind and thermodynamic structure. In experiment C1, the buoyancy is increased as in B3 and the magnitude of the shear above the low-level jet is significantly reduced, as in A7. In experiment C2, the buoyancy is increased, as in B3 and the shear is unidirectional, as in A8. In experiment C3, the buoyancy is increased, as in B3; the jet is stronger, as in A1; and the magnitude of the shear above the low-level jet is significantly reduced, as in A7. In experiments C4

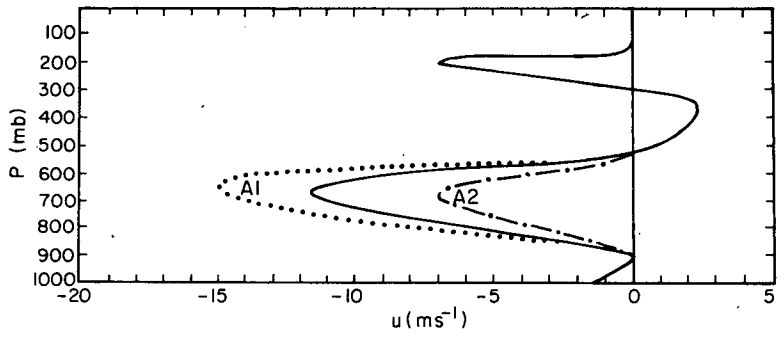

(a)

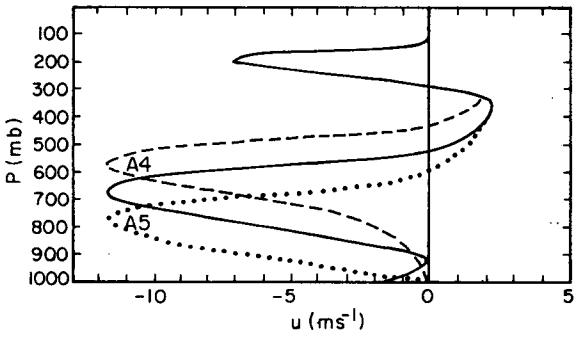

(b)

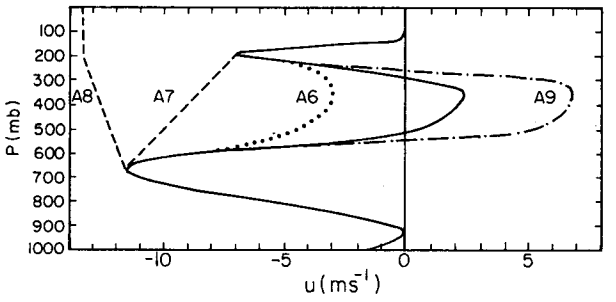

(c)

FIG. 1. Modifications to the wind profile: (a) changes to the strength of the low-level jet; (b) changes to the height of the low level jet; and (c) changes to the wind structure aloft. The solid line shows the controls wind profile.

and C5, the buoyancy is increased, as in B3; while for the former the low-level jet is stronger, as in A1; whereas for the latter it is weaker, as in A2. In experiment C6, the low-level buoyancy is increased, the jet is stronger, and there is weak shear aloft, as in A7. Finally, in experiment C6, the midlevel moisture is increased, as in B1; and the shear above the low-level jet is significantly reduced as in A7.

Initial forcing of convection is the same as that used in N87. A bubble, warmer and moister than the environment (approximately 6 km in width, 2 km in depth and centered at about 2 km above the surface),

is placed west of an applied low-level cooling rate (10 km in width and 3 km in height). The bubble is 0.5°C warmer and 2 g kg^{-1} more moist at its center than the environment and the cooling rate is 0.006°C s^{-1} applied for 15 min with a linear decrease to zero at 20 min. This produces quite a strong forcing, but was found necessary in order to overcome the detrimental effects of strong low-level shear on weakly forced convection. For all the simulations described above, the magnitude of the initial forcing is the same, although experimentation is made in some cases which will be discussed later.

4. Results

a. The control

Results for a simulation of the 12 September squall line using a 400 km domain are discussed in N87. Use of a 300 km domain, which is the size used in this study, produces very similar results. There are some differences; for instance, the mean maximum updraft velocity at 4 h is 9.7 m s^{-1} for the 300 km domain, compared to 9.2 m s^{-1} for the 400 km domain. Such a difference might be expected, considering that the simulated squall line significantly modifies the predicted fields at large distances away from the region of active convection. Clearly, a larger domain allows a more realistic feedback between the modified environment and the cloud system.

The main features of the simulated 12 September squall line, which is used as a control for the experiments, are summarized: The circulation consists of a strongly tilted updraft carrying moist boundary layer air from ahead of the system rearwards; this is undercut by a rear-to-front circulation of drier air, descending to feed the gust front and a shallow return flow near the surface. A mesolow is centered just behind the gust front at about 2 km above the surface, which apparently plays an important role in accelerating the updraft air from front to rear, and the downdraft air from rear to front. Beneath this mesolow is a shallow mesohigh, which can be accounted for hydrostatically by the cold pool formed by the downdraft air. Two broad surface mesolows occur on either side of the system associated with subsidence warming. An asymmetry in the pressure field about the region of strong convection occurs, with higher pressure generally being found ahead of the system relative to that behind. The perturbed horizontal velocity outside the region of strong convection is away from the system aloft and towards it at lower-levels. The simulated squall line is multicellular. Convective cells travel rearward relative to the gust front and eventually their updrafts become disconnected from this region of strong low-level forcing. As they migrate rearwards in the stratiform region, significant low-level perturbations in the velocity, temperature, and pressure fields occur beneath them.

b. General comparison

The simulations were run for a period of 4 h. This restricts our attention to the early stages of squall line development when convective scale processes are dominant. For reference, the results of the experiments are summarized in Table 2, which shows 1) the maximum updraft velocity, averaged between $t = 0.5$ and $t = 4$ h; 2) the maximum downdraft velocity, averaged likewise; 3) the total liquid water content in a 1 m thick section of the domain; 4) the total ice content; 5) the total precipitation; 6) the average speed of the squall line as determined from the movement of the gust front; 7) the tilt of the updraft measured anticlockwise from the horizontal. This is in some cases difficult to estimate, since the slope may change with height and because convection is often multicellular. Vertical velocity fields smoothed with a 10 km running average were used to facilitate this measurement. (One of the deficiencies of a two dimensional model is that it appears to produce updraft slopes which are less than observed); 8) the cloud top height; 9) the boundary layer cooling, estimated by averaging the temperature perturbation at the first vertical grid point (140 m above the surface), for 20 km behind the gust front; 10) the boundary layer drying, estimated likewise; and 11) the pressure difference between the surface mesohigh behind the gust front and the mesolow above it. For the readers' convenience, a summary of the results of all the experiments is provided in Table 3.

Consider first the group of experiments involving modifications of the wind profile. In one case, A3, which has no jet (initial winds are constant at 9 m s^{-1}), a long lasting system is not produced. In two other cases, A1 (stronger jet) and A4 (higher jet), the systems are extremely weak and would not be classified as squall lines. Very weak squall lines are produced in the cases of A5 (lower jet) and A10 (stronger jet with greatly reduced shear aloft). For the weaker jet, experiment A2, it is apparent that the system is less intense than the control. Maximum draft speeds are reduced, as are the boundary layer modification and propagation speed. The most noticeable difference is that the water contents are only 65% of those that occur for the control. Experiment A6, which has reduced shear above the low-level jet, produces a stronger system than that of the control environment. Updraft speeds are larger and the total water content is considerably greater. Experiment A7, for which the shear above the low-level jet is reduced further, has a similar profile to that used by Dudhia et al. (1987), to obtain a unicell circulation. This case shows dramatic differences from that of the control. Maximum updraft and downdraft speeds are considerably higher. The ice content is over three times larger for this simulation and cloud top is 2.5 km higher. Boundary layer modification is significantly reduced from that of the control and the updraft is much more vertically oriented. In experiment A8, the wind

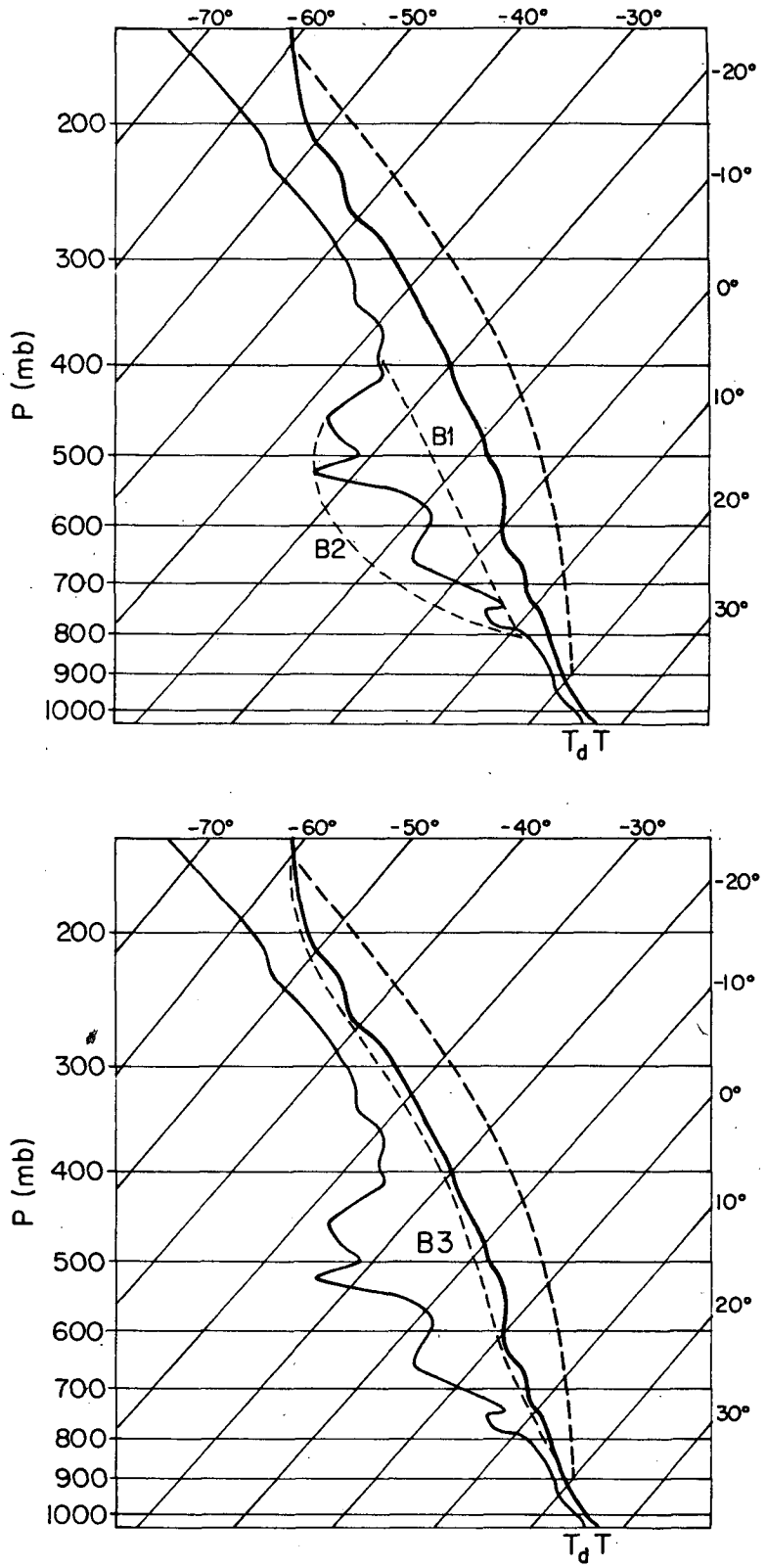

FIG. 2. Modifications to the thermodynamic structure: (a) changes to the amount of midlevel moisture; (b) increased buoyant energy; and (c) increased low-level buoyancy. The solid lines show the controls thermodynamic structure.

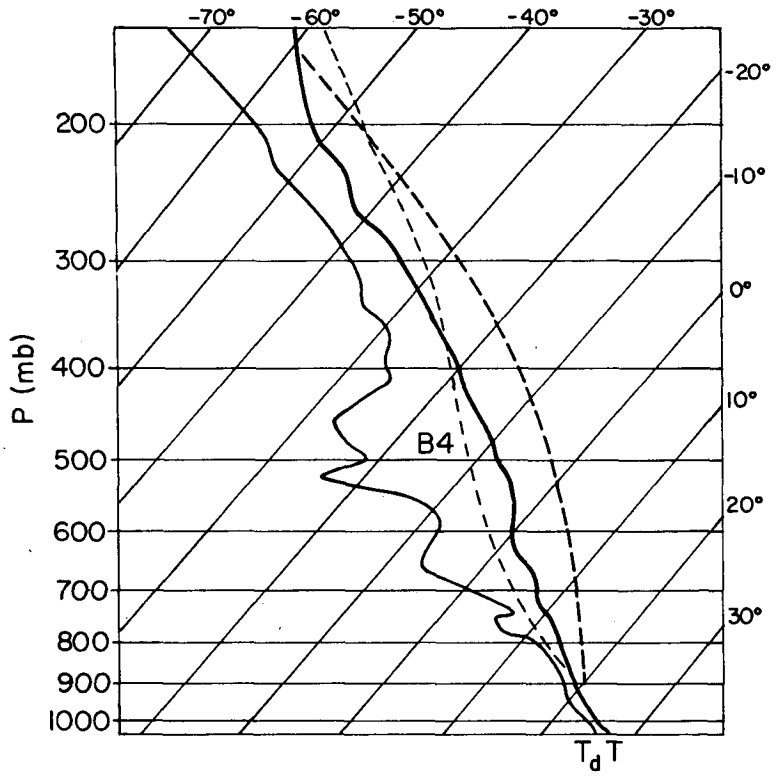

FIG. 2. (*Continued*)

shear is reduced still further, so that it becomes unidirectional. Although the maximum updraft speeds are still fairly strong, the system is weaker than the control in other respects. The updraft tilts in the opposite direction to that of the control, with precipitation tending to fall into the inflow air. Increasing the shear above the low-level jet, as in experiment A9, leads to a less intense system than the control. In summary, reducing the wind shear aloft initially leads to a more vertical, stronger updraft, increased total water content and a more unicell circulation, until the point is reached, in the case of unidirectional shear, where the system starts to become much weaker. This is consistent with the results of Thorpe et al. (1982).

The second group of experiments involve changes to the thermodynamic structure. Increasing midlevel moisture, as in experiment B1, does not make a great deal of difference. The most significant change is that the ice content is twice as large. Boundary layer cooling and drying is a little less pronounced. Although the convective instability is less, the updraft speeds are actually slightly stronger. Decreasing the midlevel moisture (experiment B2) gives trends opposite to those found for B1. It may be that dry midlevel air, although beneficial to the formation of downdrafts, due to an increased evaporation rate, has a detrimental effect on entraining updrafts. This feeds back on the boundary layer modification since weaker and drier updrafts lead to reduced rainfall rates. In experiment B3, in which the total buoyancy is increased, the system is clearly more intense. The pressure difference is significantly larger than that which occurs for the control. Somewhat surprisingly, the maximum updraft strengths are not increased by much. In experiment B4, in which the low-level buoyancy is increased it is found that the time-averaged maximum updraft strengths are only marginally increased. It is notable that the initial cell had a very strong updraft strength of 25 m s^{-1} at 25 min into the simulation. In the case of squall lines, these two-dimensional experiments do not convincingly show that the weaker updraft strengths in the GATE region compared to those over continents are primarily due to differences in the distribution of buoyancy with height. The results of these two-dimensional simulations suggest that the strong shear above the easterly jet that often exists in the GATE region, is probably a major factor inhibiting updraft strengths for squall lines.

The third group of experiments involve changes to both the wind and thermodynamic structure. The motivation for making these particular simulations arises from the results of the previous experiments. The dramatic change between the control and experiment A7, which had much weaker shear above the low-level jet, prompted simulations to find out if a similar difference occurs when the buoyant energy is increased. To get a

TABLE 2. Some general characteristics of the systems.

Group and number	Experiment	$\overline{WMAX_{up}}$ (m s^{-1})	$\overline{WMAX_{down}}$ (m s^{-1})	Total liquid water (kg m^{-1} × 10^5)	Total ice (kg m^{-1} × 10^5)	Precipitation (kg m^{-1} × 10^6)	C (m s^{-1})	Updraft tilt	Cloud top height (km)	Boundary layer cooling (°C)	Boundary layer drying (g kg^{-1})	Pressure difference (mb)
	Control	9.7	6.3	1.66	1.16	5.4	11.4	6°	12.5	−4.9	−6.2	−1.5
A1	Stronger jet	8.0	5.1	0.41	0.11	2.6	9.2	155°	5.5	−1.1	−2.0	−0.3
A2	Weaker jet	9.2	5.2	1.18	0.72	3.9	9.0	8°	12.5	−4.1	−6.2	−1.2
A3	No jet	—	—	—	—	—	—	—	—	—	—	—
A4	Higher jet	7.4	4.9	0.25	0.06	1.7	6.2	35°	5	−1.6	−2.4	−0.2
A5	Lower jet	9.3	5.6	0.71	0.37	3.7	11.2	10°	11.5	−3.0	−5.4	−0.5
A6	Reduced shear aloft	11.1	6.8	1.90	2.68	6.1	11.7	5°	14	−5.1	−6.4	−1.8
A7	Weak shear aloft	17.1	9.3	1.74	4.09	6.5	10.7	35°	15	−3.7	−4.6	−1.4
A8	Unidirectional shear	11.1	5.9	1.18	0.87	4.6	9.5	132°	12.5	−2.3	−2.7	−0.7
A9	Stronger shear aloft	9.2	5.7	1.43	0.57	4.6	10.6	4°	11.5	−4.3	−6.6	−1.2
A10	Stronger jet and weak shear aloft	9.0	5.3	0.51	0.29	3.6	9.9	90°	11	−1.1	−2.1	−0.4
B1	Increased moisture	10.5	6.0	1.81	2.7	6.3	10.6	7°	14.0	−4.3	−5.2	−1.4
B2	Decreased moisture	9.2	6.0	1.23	0.85	4.5	11.7	5°	12.5	−5.4	−6.9	−1.5
B3	Increased buoyancy	10.2	6.9	2.05	2.32	7.1	12.0	6°	15.0	−5.7	−6.3	−2.5
B4	Increased low-level buoyancy	10.1	7.2	2.37	0.93	9.0	13.0	4°	10.0	−6.2	−6.3	−2.5
C1	Increased buoyancy, and weak shear aloft	14.6	8.3	2.63	4.64	8.6	12.5	8°	15.0	−5.6	−6.0	−2.3
C2	Increased buoyancy, and unidirectional shear	15.5	8.8	2.63	5.56	9.8	12.5	8°	15.0	−5.7	−5.9	−2.1
C3	Increased buoyancy, stronger jet, and weak shear aloft	16.1	9.1	3.27	5.99	10.5	14.1	8°	15.0	−6.3	−6.3	−3.3
C4	Increased buoyancy, and stronger jet	11.4	6.7	3.32	3.44	7.7	13.2	5.5°	15.0	−6.3	−6.3	−2.3
C5	Increased buoyancy, and weaker jet	10.4	6.4	1.81	1.66	5.8	10.3	8°	14.0	−5.6	−5.6	−1.9
C6	Increased low-level buoyancy, stronger jet and weak shear aloft	14.1	8.2	4.02	2.71	12.5	13.1	5°	11.5	−7.0	−7.0	−3.3
C7	Weak shear aloft, and increased moisture	14.5	7.4	1.88	4.23	6.7	9.9	37°	15.0	−2.9	−3.8	−1.3

TABLE 3. Summary of experiments.

Experiment	Summary
A1	Stronger jet: extremely weak system, downshear tilt.
A2	Weaker jet: less intense than control, significantly reduced water content, multicellular.
A3	No jet: no system develops.
A4	Higher jet: extremely weak system, slow moving.
A5	Lower jet: very weak system, multicellular.
A6	Reduced shear aloft: stronger system than control, increased water content.
A7	Weak shear aloft: intense system, more vertically oriented updraft, strong updraft, large ice content, unicell.
A8	Unidirectional shear aloft: weak system, downshear tilt, weak boundary layer modification.
A9	Stronger shear aloft: weak system, very shallow tilt, multicellular.
A10	Stronger jet and weak shear aloft: very weak system, vertical updraft.
B1	Increased moisture: slightly more intense system than control, ice content much larger, multicellular.
B2	Decreased moisture: slightly weaker system than control, shallow tilt, multicellular.
B3	Increased buoyancy: stronger system than control, larger water content, more precipitation, multicellular.
B4	Increased low-level buoyancy: stronger system than control, low ice content, large precipitation, very shallow tilt, large boundary-layer modification.
C1	Increased buoyancy and weak shear aloft: intense system, strong updraft, large water content and precipitation.
C2	Increased buoyancy and unidirectional shear: intense system, strong updraft, large water contents and precipitation.
C3	Increased buoyancy, stronger jet and weak shear aloft: very intense system, strong updraft, very large water contents and precipitation, fast moving, large boundary-layer modification.
C4	Increased buoyancy and stronger jet: intense system, large water contents, large boundary layer modification, multicellular.
C5	Increased buoyancy and weaker jet: stronger system than control, multicellular.
C6	Increased low-level buoyancy, stronger jet and weak shear aloft: very intense system, strong updraft, very large precipitation, shallow tilt, large boundary layer modification.
C7	Weak shear aloft and increased moisture: intense system, more vertically oriented updraft, strong updraft, large ice content, weak boundary-layer modification, unicell.
D1	Control with increased cooling: very similar to control.
D2	No jet with less cooling: weak system, updrafts on both sides of system, slow moving.
D3	Stronger jet with increased cooling: slightly more intense than control, very shallow tilt, multicellular.
D4	Weaker jet with less cooling: very similar to A2.
D5	Stronger jet, weak shear aloft with increased cooling: intense system, strong updraft, large ice contents.

better idea of the relative importance of jet strength versus amount of buoyant energy on squall line propagation speed, experiments C4 and C5 are carried out. In these cases, the jet strength is altered as in A1 and A2, for increased buoyancy. In order to see if more vertically oriented stronger updrafts occur for increased low-level buoyancy, when a stronger jet with weak shear aloft is used, experiment C6 is performed. The simulation made by Dudhia et al. (1987), using a wind profile similar to that used in A7 (weak shear aloft), led to a system with only limited cooling ($\sim$1°C) at the surface, unlike the system obtained in this study. The sounding they used was very moist, so to see if this is the major factor responsible for this difference, experiment C7 (weak shear aloft and increased mid-level moisture) is carried out.

Experiment C1, has weak shear aloft, as in A7, and increased buoyancy. One might expect stronger updraft strengths due to the increased buoyancy and a more vertical updraft than occurs in A7. However, draft strengths are actually less and the updraft more tilted from the vertical. Although maximum draft strengths are not as large as those in A7, in other respects this system is more intense. It seems that the increased buoyancy produces a cooler, deeper cold pool and stronger warming above. The faster movement of this cold pool and the increased front-to-rear acceleration of the updraft air associated with the enhanced mesolow, possibly accounts for the more tilted updraft. In experiment C2, in which the buoyancy is increased for unidirectional shear, an intense system, very similar in most respects to C1 is obtained. In experiment C3, the buoyancy is increased, the jet is stronger and the shear aloft is greatly reduced. This produces a very intense system. However, the updraft is still more tilted from the vertical than occurs for A7 (weak shear aloft). This system is the fastest moving of all the cases. Experiment C4, in which the buoyancy is increased for a stronger jet produces an intense system. The speed of this system is slightly faster than for B3, which had the standard jet and increased buoyancy. As might be expected, experiment C5, in which the buoyancy is increased for a weaker jet, produces a system with a slightly slower propagation speed than B3. Experiment C6, which has increased low-level buoyancy, a stronger jet and greatly reduced shear aloft, produces a very intense system. Updraft strengths are much stronger than for A10, which has the same wind profile, but the standard distribution of buoyancy with height. However, A10 is a very weak system because the initial forcing is not large enough to overcome the detrimental effect of the increased low-level shear on the convection. More will be said about this later. The boundary layer modification is extremely large for this squall line. Considering how cool the cold pool is, this system moves surprisingly slowly.

Experiment C7, has weak shear aloft and increased moisture. The time-averaged maximum draft strengths

are weaker than for A7 (weak shear aloft), which is contrary to what one might expect from experiments B1 and B2. These cases, which use the standard wind profile, suggest increased moisture leads to a more intense system. Not surprisingly, the moister midlevel air which tends to inhibit evaporation leads to less boundary layer cooling and drying. However, the cold pool is still significantly cooler than occurs in Dudhia et al.'s simulation. The environment they used is even moister than used here; however, the major difference is that the nighttime sounding they used has a more stable layer near the surface. This was responsible for the lowest inflow air rising slightly at the front of the system but then descending back to the surface. We experimented with using a stabler lower layer, and were able to obtain a squall line without a significant cold pool; however, the intensity of the system was much weaker. The time-averaged draft strengths for C7 are less than for A7, because the system is weaker in the early stages. This appears to be related to the reduced boundary layer cooling resulting from the increased midlevel moisture. This leads to a more downshear tilted updraft relative to the low-level winds. Water loading and evaporation inhibit development, until the updraft establishes an upshear tilt.

In general, the more intense systems have a larger pressure difference between the surface high and the mesolow above, the exception being the unicell systems with more vertically oriented updrafts (A7 and C7). These cases which are intense in the sense of having large updraft strengths, both possess relatively weak cold pools.

In order to get some idea as to the sensitivity of the simulations to the initial forcing, additional experiments were made. In particular, it appears that in some cases forcing is either too strong or too weak for an organized deep convective system to develop. In the cases of A3 (no jet) and A4 (higher jet), it seems that the initial forcing is too strong. The cold pool surges ahead of the initial thermal, hence decoupling the region of strong upward forcing from the main updraft. On the other hand, for cases A1 (stronger jet) and A10 (stronger jet with greatly reduced shear aloft), the systems updraft tilts downshear relative to the low-level flow allowing precipitation to fall into the inflow. This suggests the initial cold pool is not strong enough to produce an upshear tilt. We were unable to obtain a deep convective system in the case of A4 (higher jet), but were successful for the other cases. The wind profile for experiment A4, has weak shear below 2 km, but strong shear above (see Fig. 1b). According to Rotunno et al. (1988), small low-level wind shear requires a weak cold pool to produce optimum lifting at the gust front. On the other hand, strong shear aloft in the absence of other vorticity sources and sinks, is detrimental to thermals. Hence, if the cold pool is weak, the convection is not forced enough to overcome the detrimental effects of strong shear aloft. However, if the cold pool

TABLE 4. Some general characteristics for cases with altered initial cooling rates.

Group and number	Experiment	$\overline{WMAX_{up}}$ (m s^{-1})	$\overline{WMAX_{down}}$ (m s^{-1})	Total liquid water (kg m^{-1} × 10^5)	Total ice (kg m^{-1} × 10^5)	Precipitation (kg m^{-1} × 10^6)	C (m s^{-1})	Updraft tilt	Cloud top height (km)	Boundary layer cooling (°C)	Boundary layer drying (g kg^{-1})	Pressure difference (mb)
D1	Control											
	Increased cooling	9.2	5.6	1.52	1.25	5.1	11.1	5°	12.5	−4.7	−6.3	−1.3
D2	No jet, less cooling	10.7	5.7	0.89	0.86	2.9	2.7	11°	12.5	−2.7	−4.9	−0.6
D3	Stronger jet, increased cooling	9.7	6.6	1.69	1.37	5.7	12.4	5°	12.5	−5.1	−6.3	−1.6
D4	Weaker jet, less cooling	9.5	5.7	1.22	0.82	3.9	9.2	7°	12.5	−4.4	−6.4	−1.1
D5	Stronger jet, weak shear aloft, increased cooling	16.7	9.7	2.3	5.1	8.7	13.0	17°	15.0	−4.9	−6.3	−2.0

is strong, instead of forcing deep uplift, the inflow is swept rearwards over the gust front. A possible contributing factor inhibiting convection, which was observed for both the no-jet and high-jet cases (in the case of strong forcing), may have been the advection of a layer of more stable air, due to compensating subsidence ahead of the initial thermal, over the gust front.

Table 4 shows results for experiments in which the magnitude of the applied cooling rate is altered from the standard value of 0.006°C s^{-1}. Increased cooling refers to a rate of 0.008°C s^{-1} and decreased cooling to a rate of 0.002°C s^{-1}. In addition to the cases previously mentioned, experiments were carried out for the control environment, with stronger forcing (D1), and the weaker jet environment, with less forcing (D4). In these two cases, no significant differences occur from the standard forcing experiments. However, in the other cases, significant differences do occur. In experiment D2, which has no wind shear, reduced forcing allows a weak but organized and persistent system to develop. (In order to keep this slowly moving system in the center of the domain, the constant wind speed is decreased from 9 to 2 m s^{-1}.) In experiments D3 (stronger jet) and D5 (stronger jet with weak shear aloft) quite intense systems are obtained when the initial forcing is increased. These experiments suggest that although the initial forcing can be either too strong or too weak for an organized system of deep convective cells to develop, there is a fairly broad range of forcing, for which system characteristics are relatively insensitive.

c. *Description of individual cases*

There are too many experiments to describe them all in detail. We discuss four, which illustrate many of the basic features of these systems.

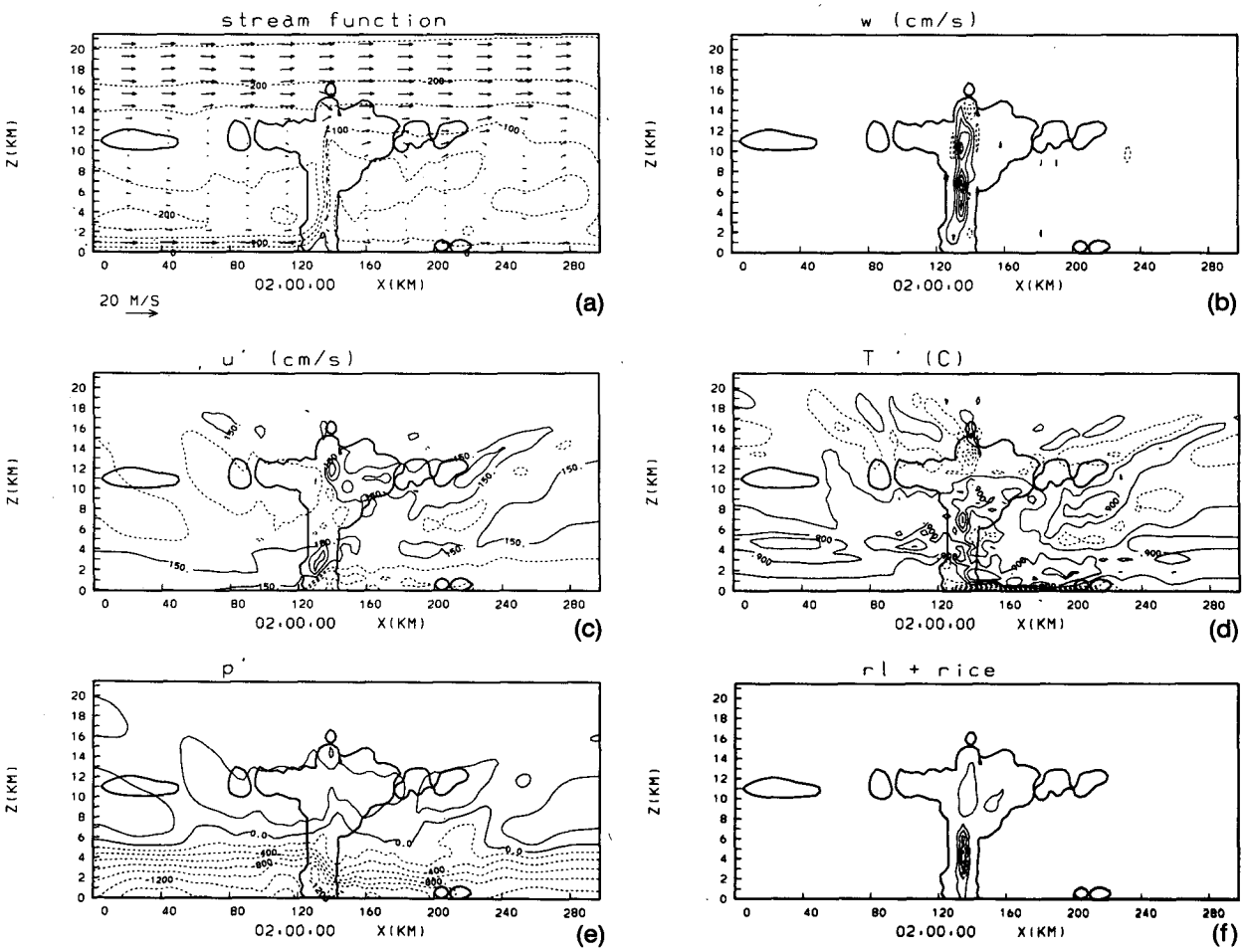

FIG. 3. Number A7 with weak shear aloft, at 2 h: (a) Velocity vectors and streamlines. The contour interval is 500 $m^2 s^{-1}$, and the label scale is 10^{-1}. (b) Vertical velocity. The contour interval is 150 cm s^{-1}. The dashed contour indicated downward motion. The contours begin at ±75 cm s^{-1}. (c) Horizontal velocity perturbation. The contour interval is 300 cm s^{-1}. Dashed contours indicate flow from right to left. (d) Temperature perturbation. The contour interval is 0.6°C. Negative values are indicated by dashed lines. (e) Pressure perturbation. The contour interval is 20 Pascals and the label scale is 10. (f) Liquid and ice water mixing ratio. The contour interval is 1.5 g kg^{-1} and the label scale is 100.

1) A7: WEAK SHEAR ALOFT

Figures 3a–f show fields of streamfunction and velocity vectors, vertical velocity, perturbation horizontal velocity, perturbation temperature, perturbation pressure, and liquid and ice water content, respectively, at 2 h. The cloud outline which includes rain water, is also contoured in these figures. The updraft is vertical above 3 km. There is strong deceleration of the horizontal velocity of the inflow air as it ascends over the gust front. A large horizontal pressure gradient responsible for this deceleration is evident in Fig. 3e. Subsidence warming occurs on either side of the system. At low levels it is more prevalent behind the system, just above the cold pool. The largest water contents occur between 2 and 7 km above the surface. There is only a weak mesolow just behind the leading edge at the interface between the cold pool and the warm air above, at 2 h. Figures 4a–f show fields at 4 h. The updraft is tilted at 4 h and its magnitude has weakened. Downdrafts feeding the cold pool are stronger than at 2 h. A pronounced mesolow now occurs just behind the leading edge at the interface between the cold pool and the warmer air above. Inflow air is accelerated as it begins to ascend over the gust front but subsequently is decelerated. However, a considerable horizontal component of momentum is maintained by the updraft air. The water contents in the anvil are much more homogeneous than occur for the control (not shown) and there is little evidence of multicellular behavior.

The propagation speed is fairly constant, increasing by only ≈ 1 m s^{-1} during the simulation. The cold pool becomes deeper and cooler at a gradual rate (until 3.5 h) after which quite a significant change occurs. Rotunno et al. (1988) determine the optimum condition for uplift due to a cold pool interacting with a sheared flow, to be attained when

$$\Delta u = \left(-2g \int_0^H \frac{\theta_v'}{\theta_{v0}}\, dz\right)^{1/2} \tag{1}$$

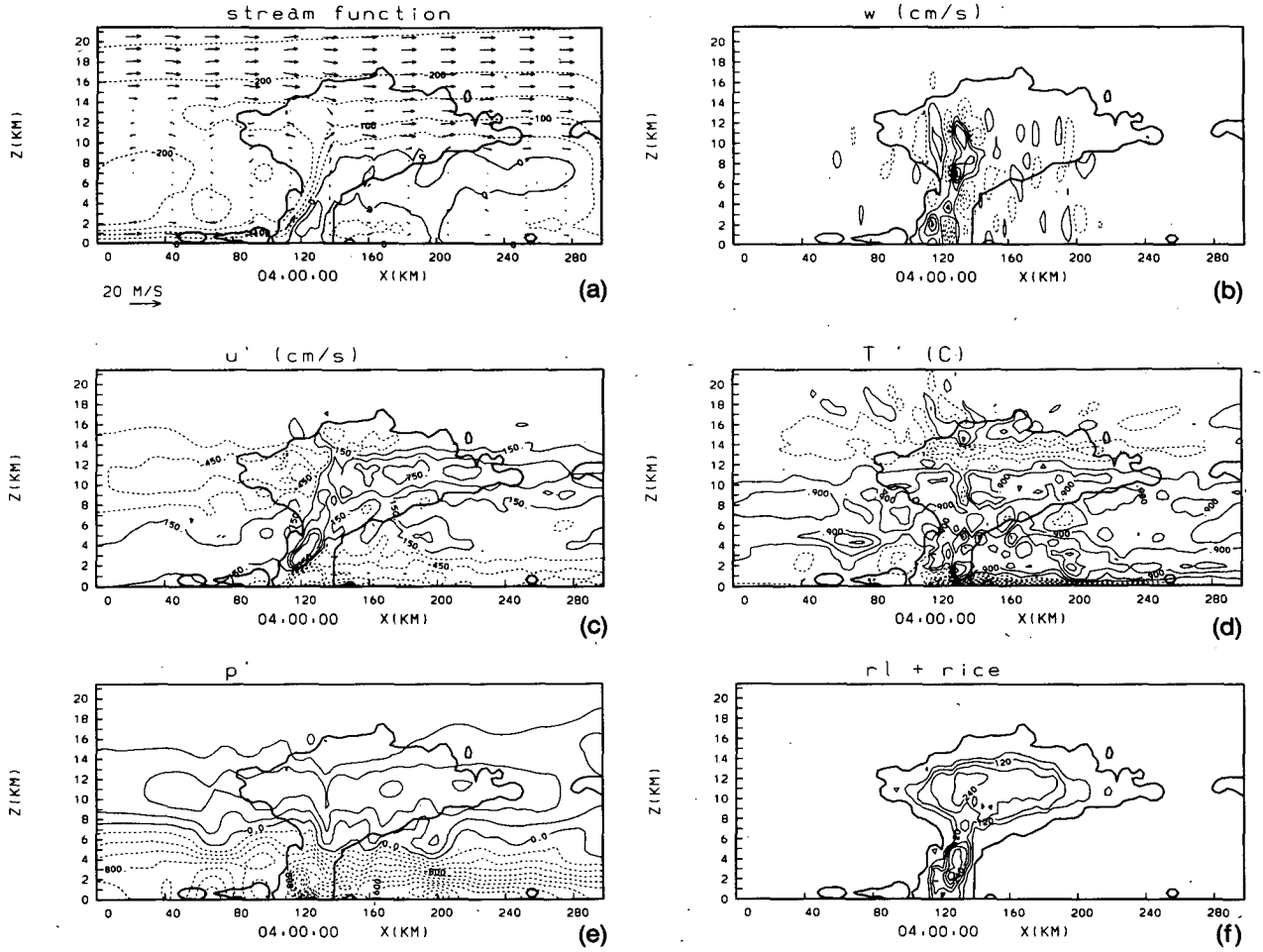

FIG. 4. As in Fig. 3 except at 4 h and the contour intervals are 100 cm s^{-1} for the vertical velocity and 0.6 g kg^{-1} for the liquid and ice water mixing ratio.

where Δu is the velocity difference between the surface and the height where the updraft exits as a vertical jet, θ_v' is the perturbation virtual temperature and H the height of the cold pool. Averaging θ_v' for 10 km behind the gust front at each level in the cold pool, we find $\Delta u = 7.6$ m s^{-1} at 2 h, in reasonable agreement with the observed value and $\Delta u = 14.8$ m s^{-1} at 4 h. At 4 h, the required Δu is considerably larger than actually exists and hence the updraft is tilted. However, we will examine the vorticity balance that occurs for this system in more detail in section 4e, and show that a somewhat different interpretation of the optimum condition is required. The unicell circulation obtained in this two-dimensional simulation may possibly be found in actual squall lines, either as a long-lived line section or as persistent cells. The right combination of conditions required for a unicell would make them a rare event. The steadiness of the circulation is to some degree dependent on the details of the microphysical parameterizations. For instance, if the fallout of ice particles were larger, this would adversely effect the updraft leading to a less steady circulation. Clearly more knowledge is required of the microphysical processes that occur.

2) C3: Increased buoyancy, stronger jet, reduced shear aloft

In this increased buoyancy simulation, the wind profile below 650 mb is the same as in A1 and the wind shear above this level is reduced as in A7 (see Fig. 1). Figures 5a, b, c, d, e, and f, show fields at 3.5 h. There is a strong low-level rear inflow into the system. The updraft air, as well as exiting to the rear at upper-levels, also feeds a pronounced forward overhanging anvil. The perturbation velocity shows the winds ahead of the system are significantly modified from that of the initial environment. The temperature field shows a

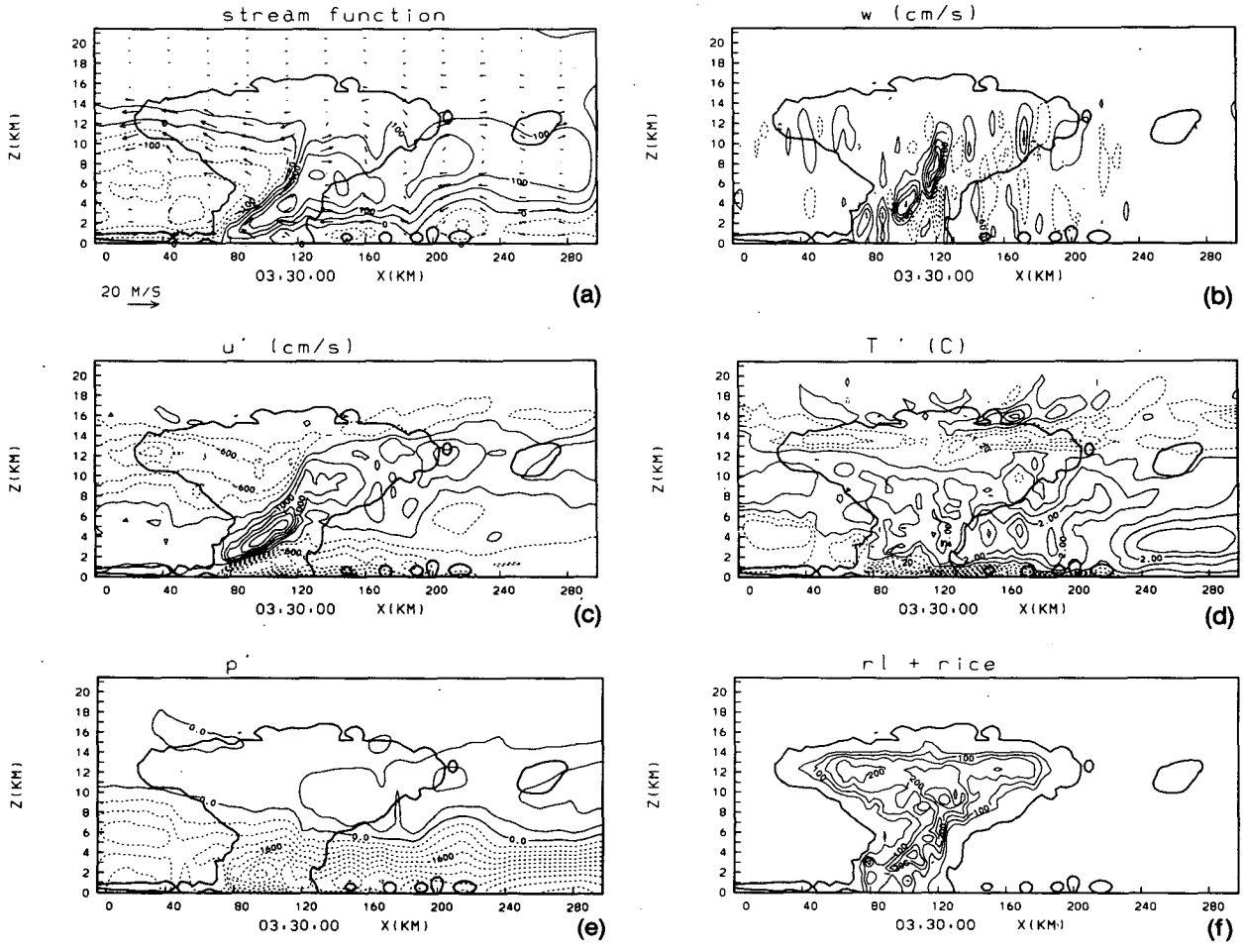

FIG. 5. Number C3 with increased buoyancy, stronger jet, and weak shear aloft, at 3.5 h: (a) Velocity vectors and streamlines. The contour interval is 500 m^2 s^{-1} and the label scale is 10^{-1}. (b) Vertical velocity. The contour interval is 120 cm s^{-1}. (c) Horizontal velocity perturbation. The contour interval is 400 cm s^{-1}. (d) Temperature perturbation. The contour interval is 0.8°C. (e) Pressure perturbation. The contour interval is 40 Pascals and the label scale is 10. (f) Liquid and ice mixing ratio. The contour interval is 0.5 g kg^{-1} and the label scale is 1000.

deep cold pool. Low-level subsidence warming is particularly large behind the system. Ahead of the system, cooling has occurred at low levels. Pressure anomalies are very large at the rear of the system. However, the limited domain size prevents drawing definite conclusions regarding the modification ahead of the squall line. To overcome the uncertainties associated with a small domain size, a simulation with this environment was carried out using a 1000 km domain and a 1 km horizontal grid resolution. This confirmed that the pressure anomalies are indeed larger behind the system (not shown).

The transition from a vertical to a tilted updraft occurs earlier in this case than for A7 (weak shear aloft), discussed previously. However, apart from this and the difference in magnitude of the changes that occur, the basic structure of the systems are very similar. A squall line of this intensity is unlikely to be found over the tropical oceans, but is not excessively strong for systems that occur over land, in West Africa, or at midlatitudes.

3) D2: No jet and less cooling

As discussed earlier, this simulation has no wind shear (environmental winds are constant at 2 m s^{-1}) and the initial cooling rate has been considerably reduced. Fields of streamfunction and vertical velocity at 4 h are shown in Fig. 6a and b, respectively. Unlike the other cases, significant updrafts occur on either side of the system, which feed a common anvil. The updraft on the left hand side of the domain dominated early on in the simulation, but became progressively more tilted and weaker as time went on. The updraft on the right-hand side is far more upright at 4 h, while on the other side of the system the convection has more of a multicellular appearance. The left-hand side updraft traverses to the far right-hand side of the system, where it encounters updraft air ascending over the other gust front. It is possible this plays a role in maintaining the very upright right-hand side updraft. This updraft can be eliminated by introducing a shallow dry pool into the initial environment (4 g kg^{-1} drier at the surface, linearly decreasing to zero at a height of 2 km), extending from the middle of the domain to the right hand boundary. Fields at 2.5 h for this simulation, using a smaller 100 km domain, are shown in Fig. 7. The structure of this system is very similar to those discussed previously, although much weaker. It is interesting to compare this system with the slow moving convective line studied by Zipser et al. (1981) and LeMone (1983). The mesolow above the surface is of the same magnitude as for the observed system. However, the simulated system is much more tilted and the momentum fluxes occur at a lower level (not shown). Unlike the observed convective line there is a significant cold pool. These differences are probably attributable to differences in environmental structure and the three-dimensional structure of the observed system. The observed convective line formed in a less unstable environment which was much moister at mid levels. This is likely to inhibit the development of a deep cold pool. Furthermore, the convective line aligned parallel to the mean wind shear and cells had a tendency to form near the one end of the line and dissipate at the other.

The simulated system formed in an environment with no preexisting shear. Its effect is to generate shear. This is consistent with the results of Soong and Tao (1984) who also obtain countergradient momentum transport for an environment having weak low-level wind shear perpendicular to the convective line. In contrast, most of the other more intense cases act to reduce the mean low-level wind shear. However, there is no fundamental difference in structure between these two types of systems. The reason most cases reduce the wind shear is because shear interacting with a cold pool favors updrafts on a particular side of the system. The updraft tilts upshear relative to the low-level environment winds. The resulting momentum transports cause the flow aloft to be increased while the flow at low levels is decreased, reducing the wind shear. In the no-shear case, in which the right-hand side updraft was removed by the introduction of a shallow dry pool, the system did exactly the same thing in the sense that updraft air was accelerated from front to rear, while downdraft air was accelerated from rear to front. In the absence of any preexisting environmental shear, this results in the generation of shear. In terms of the

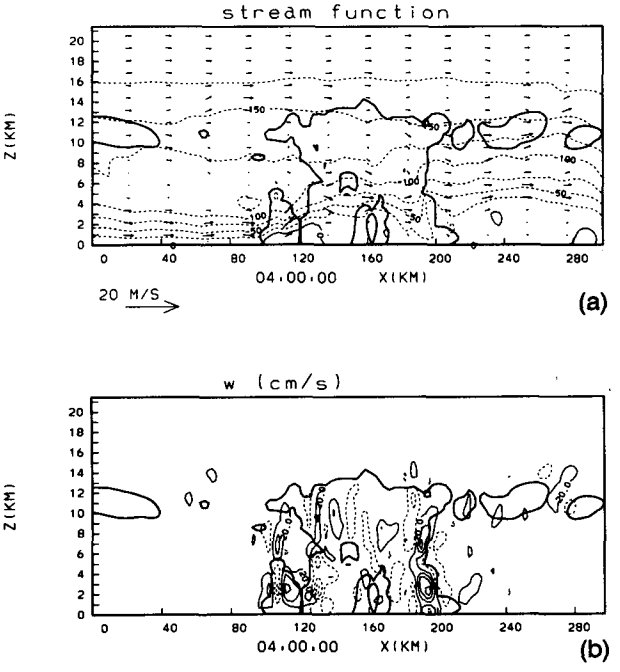

FIG. 6. Number D2 with no shear and less cooling, at 4 h: (a) Velocity vectors and streamlines. The contour interval is 250 $m^2 s^{-1}$ and the label scale is 10^{-1}. (b) Vertical velocity. The contour interval is 40 cm s^{-1}.

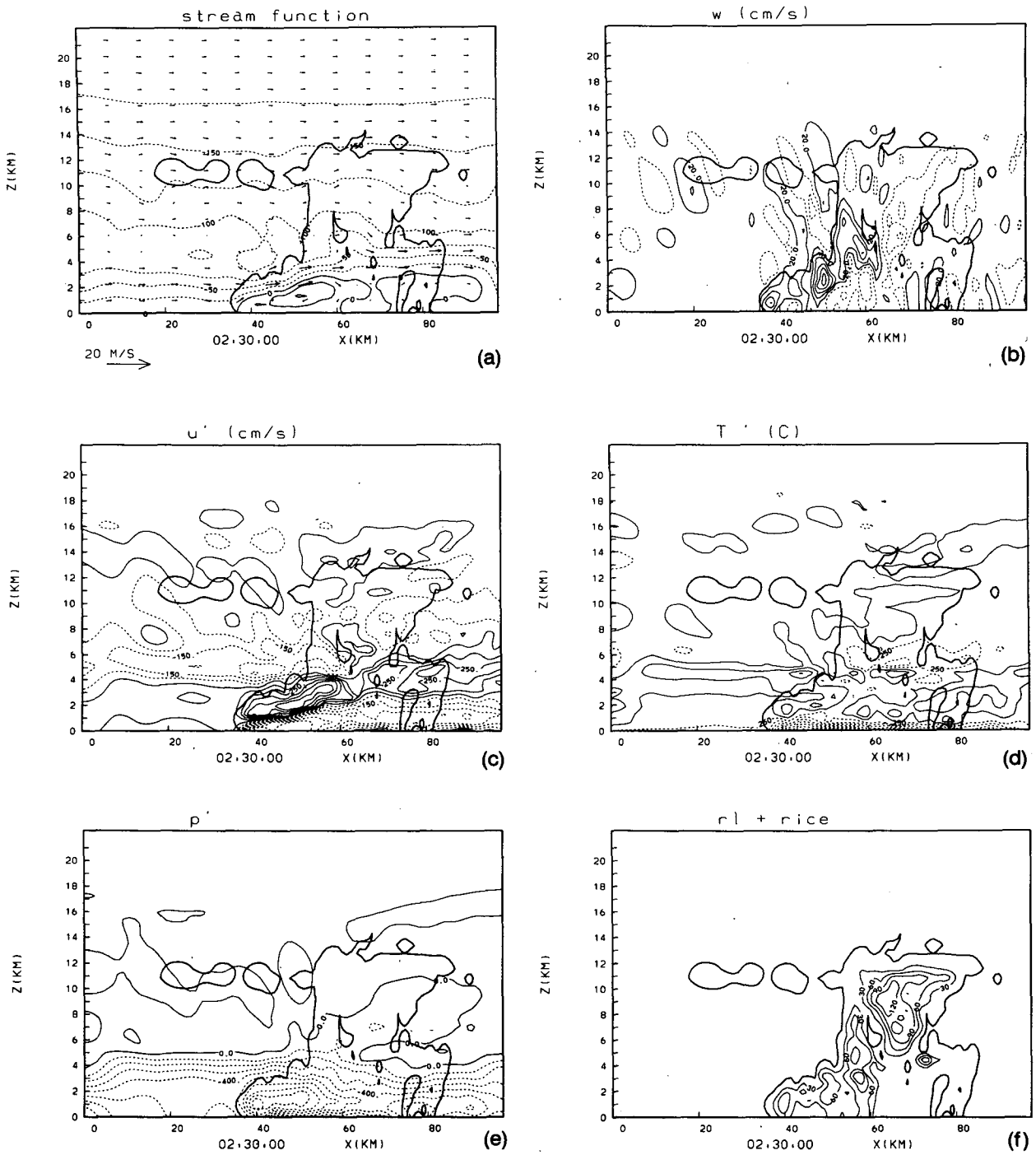

FIG. 7. No shear, less cooling and shallow dry layer, at 2.5 h: (a) Velocity vectors and streamlines. The contour interval is 250 $m^2 s^{-1}$ and the label scale is 10^{-1}. (b) Vertical velocity. The contour interval is 40 cm s^{-1}. (c) Horizontal velocity perturbation. The contour interval is 100 cm s^{-1}. (d) Temperature perturbation. The contour interval is 0.5°C. (e) Pressure perturbation. The contour interval is 10 Pascals and the label scale is 10. (f) Liquid and ice water mixing ratio. The contour interval is 0.3 g kg^{-1} and the label scale is 1000.

energy transformation framework presented by Asai (1964), the no-shear case has increased the mean horizontal kinetic energy, whereas the squall lines which form in significant low-level shear have produced a decrease in the mean kinetic energy. Whether the transformations of mean kinetic energy contribute significantly to the total energy budget has yet to be determined.

4) A5: LOWER JET

The weak intensity of A5 is related to the strong shear above the jet. The inflow is turned by the cold pool so that it has a considerable vertical component. However, as the updraft encounters the relatively faster moving winds above the low-level jet it becomes more tilted. The horizontal acceleration of the updraft air above the low-level jet is due to a pressure gradient, probably dynamic in origin. Following Rotunno and Klemp (1982), the linearized diagnostic pressure equation, neglecting buoyancy effects can be written

$$\nabla^2 p' = -2 \frac{\partial w}{\partial x} \frac{dU}{dz} \tag{2}$$

where U is the basic state horizontal velocity. For a single Fourier component, the Laplacian of the function is negatively proportional to the function itself. Hence, qualitatively, we might expect

$$p' \sim \frac{\partial w}{\partial x} \frac{dU}{dz}. \tag{3}$$

Therefore, one might anticipate the updraft to develop a high pressure on the upshear side as it encounters the strongly positively sheared winds above the low-level jet. The updraft shears off until it reaches a point where it breaks away from the low-level forcing. This continually happens so that the system is multicellular. In cases where the jet is at the standard height and there is strong positive shear above, high pressure also develops at midlevels ahead of the system (as discussed for the control case in N87). In these cases the detrimental effects of the strong shear occur higher and are less disruptive to the system as a whole.

The results obtained from two-dimensional numerical experiments concerning the effects of strong shear aloft, and, in particular, its influence on the multicellular character of these systems must be viewed with caution at this stage.

d. General properties

1) STRUCTURE

For the most part, differences in structure are more of degree than of kind. Much of the structure of the squall lines is similar to the symmetrical response that might be expected of a nonsheared atmosphere to midlevel warming and low-level cooling. The effect of midlevel warming by itself, is to produce high pressure above and a low beneath, which opposes the upward motion. This causes air to be accelerated away from the warming region aloft and towards it below. Compensating subsidence occurs in the air outside the warming region. Superimposed on this is the effect of low-level cooling which produces a cold pool. The high pressure at the surface caused by the cooling separates the broad surface low which would exist in its absence, into two lows on either side of the system. Furthermore, a low pressure exists at the cold/warm air interface which has its largest magnitude relative to the environmental air at the same level, where the vertically integrated buoyancy above is a maximum. This response is most pronounced for systems which develop an upshear tilt (relative to the low-level winds), since in this situation, warming occurs above a cooling region. Moreover, for a vertical updraft, the hydrostatic lowering of pressure due to warming is countered to a certain extent by the effects of waterloading, as will be shown in subsection 4d2.

A common feature is a band of warm air overlying the cold pool. A simulation in which a cold pool is formed by an applied cooling rate (using the control environment) with the microphysics switched off, also shows this feature. Low pressure forms at the top of the cold pool, which not only drives horizontal convergence required to feed the downdraft, but also causes subsidence. (This low pressure is consistent with the buoyancy field but may also have important dynamic contributions.) This subsidence warming atop the cold pool extends far outside the applied cooling region. It is quite possible that this is related to the fact that the rear inflow in these simulations usually remains warmer than the environment as it descends beneath the stratiform region.

As might be expected, deeper updrafts tend to produce subsidence warming through a greater depth of the atmosphere. Systems with a vertically oriented updraft are inclined to give rise to as much warming ahead of the system as behind, whereas systems with an upshear tilted updraft (relative to the low-level winds) tend to have more warming to the rear. Pressure anomalies are consistent with this. A feature of simulations which have strong positive shear above the low-level jet is that high pressure tends to occur ahead of the system at midlevels. A possible reason for this was discussed previously for experiment A5, the lower jet. A noticeable characteristic of vertical updrafts is that there is apt to be a fairly symmetrical surface mesolow ahead of the system, of greater magnitude than occurs behind. This same feature is seen in the early stages of most of the simulations, when the updraft is more upright. Lin (1987) investigated the linear response of the atmosphere to diabatic heating. He found that the surface low pressure pattern was strongly influenced by the presence of shear. We performed a numerical experiment using a dry atmosphere, where the heating rate was applied in a vertical column in the presence of low-level shear. The lowest surface pressure did indeed occur ahead of the heated region. This is also consistent with the low-level pressure anomaly predicted by Eq. (3).

Gravity waves are observed to emanate from the systems. A primary mechanism for forcing these waves seem to be overshooting thermals. However, other forcing mechanisms exist. For example, the first major

gravity wave is evident in the simulations at about 45 min, a consequence of the downdraft produced by the initial thermal causing a surge in the gust front. This creates enhanced low-level convergence on either side of the system and forces a deep gravity wave. As gravity waves travel away from the system, perturbations associated with them become broader and weaker in magnitude. There is some indication that gravity waves are partially trapped by the cool layer that exists at cloud top (presumably a consequence of overshooting). It was suggested by Lindzen and Tung (1976) that a more unstable layer of air can produce this effect, and was suggested by Tripoli (1986) in relation to the anvils of mesoscale systems. Gravity waves are probably exaggerated in simulations where vertical motions are confined by two-dimensional geometry. Furthermore, along a squall line convective cells are likely to be in different stages of development and hence the gravity waves produced by them might only occasionally interfere constructively.

2) PROPAGATION SPEED

In all the simulations in this study, a cold pool is produced. The main updraft is forced at low levels by convergence at the gust front which in these simulations is at the head of the cold pool. Hence, it is likely that the speed of the system is related to the speed of a density current. In this section, an attempt is made to determine how accurately the density current model predicts the speed of the gust front. It is important here to differentiate between a "gust front," which is a generic convergence line associated with a thunderstorm, and a "density current," which is a type of gust front, originating from the density contrast between a cold pool and its environment. The speed of a density current has been derived theoretically by Benjamin (1968) and, in a particularly simple manner, by Rotunno et al. (1988), who obtained

$$C = \left(-2g \int_0^H \frac{\theta_v'}{\theta_{v0}}\, dz\right)^{1/2} \tag{4}$$

where θ_v' is the perturbation virtual potential temperature from the basic state value θ_{v0} and H the height of the density current. For the results to be presented, θ_v' is averaged at each grid level in the density current, for 10 km just behind the gust front. Table 5 shows the predicted propagation speeds between 3 and 4 h estimated as the average of the values determined at these two times. The speed is given relative to the surface. The predicted speed is assumed to be relative to the environmental winds in the lowest level, which in most cases move at -1.3 m s^{-1} relative to the surface. Appropriate corrections have been added to the propagation speeds. Also tabulated is the simulated propagation speed relative to the surface between 3 and 4 h. The simulated propagation speed is plotted against the predicted speed in Fig. 8. Although there is broad agreement in the respect that systems having cooler and deeper cold pools tend to move faster, there are some significant differences. Almost all the systems

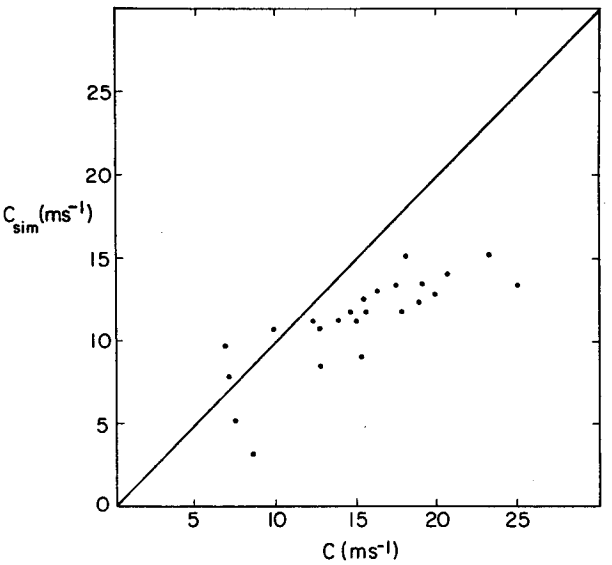

FIG. 8. Plot of simulated propagation speed (C_{sim}) between 3 and 4 h against predicted propagation speed (C).

TABLE 5. Predicted propagation speed of systems according to Eq. (4) (C) and simulated (C_{sim}).

Group and no.	Experiment	C	C_{sim}
	Control	15.5	12.5
A1	Stronger jet	7.1	7.9
A2	Weaker jet	12.9	8.4
A4	Higher jet	7.5	5.1
A5	Lower jet	12.4	11.2
A6	Reduced shear aloft	15.6	11.8
A7	Weak shear aloft	14.0	11.2
A8	Unidirectional shear	9.9	10.7
A9	Stronger shear aloft	15.0	11.2
A10	Stronger jet and weak shear aloft	6.9	9.6
B1	Increased moisture	14.7	11.8
B2	Decreased moisture	16.4	12.9
B3	Increased buoyancy	17.9	11.8
B4	Increased low-level buoyancy	19.9	12.9
C1	Increased buoyancy and weak shear aloft	18.9	12.3
C2	Increased buoyancy and unidirectional shear	20.7	14.0
C3	Increased buoyancy, stronger jet, and weak shear aloft	23.1	15.1
C4	Increased buoyancy and stronger jet	19.1	13.4
C5	Increased buoyancy and weaker jet	15.3	9.0
C6	Increased low level buoyancy, stronger jet, and weak shear aloft	25.0	13.4
C7	Weak shear aloft and increased moisture	12.8	10.7
D2	No jet and less cooling	8.6	3.1
D3	Stronger jet and increased cooling	17.5	13.4
D5	Stronger jet, weak shear aloft, and increased cooling	18.9	15.1

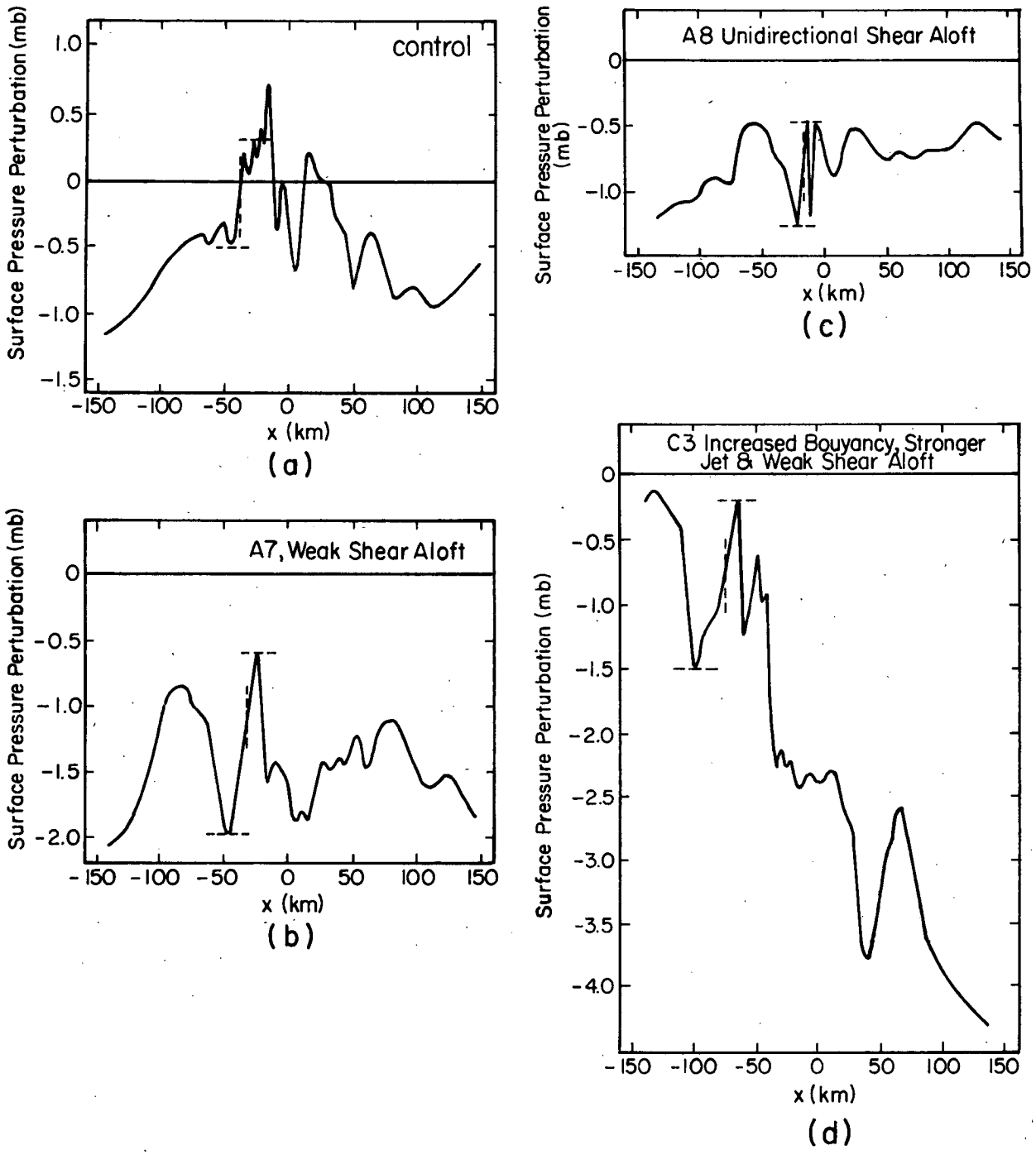

FIG. 9. Surface pressure perturbations at 3.5 h: (a) Control, (b) A7 with weak shear aloft, (c) A8 with unidirectional shear aloft, (d) C3 with increased buoyancy, stronger jet, and weak shear aloft, (e) C6 with increased buoyancy, stronger jet, and weak shear aloft, and (f) with no jet and less cooling. The horizontal dashed lines indicate the estimated pressure jump across the gust front. The vertical dashed line indicates the leading edge of the density current.

tend to move slower than the predicted speed, except for three cases. These systems, A1, A8, and A10 are very weak and have a tendency to tilt downshear except at very low levels.

There appear to be three main reasons why the actual propagation speed differs from that predicted by Eq. 4. The first of these is that Eq. 4 does not take into account the effects of viscosity. Benjamin (1968)

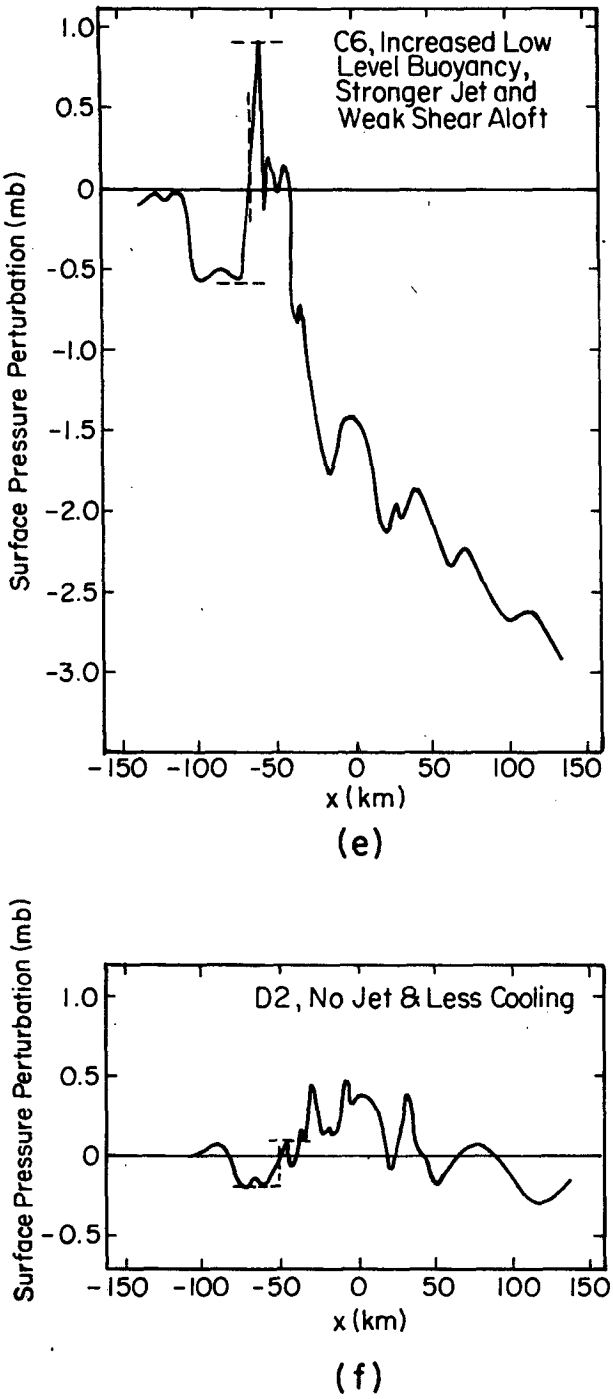

FIG. 9. (*Continued*)

showed that the internal Froude number k is equal to 1.414, for two immiscible, inviscid fluids. This corresponds to the factor 2 which occurs under the square root in Eq. (4). Values of k obtained for atmospheric density currents range from $k = 0.70$ to $k = 1.08$ (Wakimoto 1982). If a value of $k \sim 1$ is used in Eq. 4, then considerably better agreement with the observed speeds can be obtained in the majority of cases. However, for the three systems which move faster than predicted by Eq. (4), agreement is made worse. Furthermore, some of the systems which move much more slowly than predicted by Eq. (4), in particular D2 and C6, still show significant differences.

The second reason is that acceleration of the low-level environmental winds ahead of the gust front can occur, which changes the surface relative propagation speed. Acceleration of low-level winds toward the system normally occurs at large distances ahead of the squall line. However, just in front of the gust front, there is often acceleration of air away from the system, towards the surface mesolow ahead of it.

Finally, the gust front is driven by the pressure gradient force. It turns out that the virtual potential temperature difference in the cold pool from that of the environment does not always provide an accurate means of estimating this. Seitter (1986) in a modeling study used a modified equation based on the surface pressure difference across the gust front,

$$C_p = k\left(\frac{\Delta P}{\rho_w}\right)^{1/2} \tag{5}$$

where ΔP is the pressure difference and ρ_w the density of the air in the cold outflow. Seitter obtained more accurate predictions for the propagation speed using this formula. In particular, it was found that when clouds occur above the cold pool, the release of latent heat and associated warming led to a reduced pressure difference and hence propagation speed.

We attempted to determine the propagation speed including the aforementioned effects. Figures 9a–f show the surface pressure fields for six of the systems, at 3.5 h. It is apparent that it is not always an easy task to determine the pressure jump across the cold pool. There is no constant environmental pressure, followed by an abrupt jump to a constant post gust front pressure. However, there is often a pronounced minimum just ahead of the gust front and a maximum just behind. We assume that it is this peak-to-peak pressure jump (the difference between the horizontal dashed lines) that occurs in close proximity to the gust front (indicated by a vertical dashed line) to be the relevant pressure difference. In ambiguous cases, such as the control, the estimated surface pressure jump is also based on earlier and later pressure fields. It is possible that in three dimensions, the fields would be smoother. For instance, the perturbations due to gravity waves are likely to be exaggerated in two-dimensional simulations. The low-level wind modification is estimated by averaging the winds at the lowest level for 10 km, centered at 10 km ahead of the gust front, at 3.5 h. This should be regarded as only a rough approximation, since winds in this region can vary significantly in an hour, depending on the simulation.

The Froude number used in Eq. 5 is $k = 1.1$. This value is chosen so as to provide the best agreement between simulated and predicted speeds. Dry simulations, initialized using cooling rates to produce a density current, were carried out for various environmental profiles. A value of $k = 1.1$ also produces reasonable agreement with the results of these dry simulations. It is worth mentioning that Eq. (5) can be obtained from the steady state inviscid horizontal momentum equation applied at the surface, as in Raymond (1975). Integrating this equation from ahead of the gust front to a point where a stagnation point exists (in a coordinate system moving with the gust front), a balance is obtained between the square of the surface inflow speed and the pressure jump. It is not obvious how one should interpret the parameter k in Eq. 5, which in Eq. 4 is commonly viewed as a correction necessitated by the effects of internal viscosity and surface friction. One reason that it is less than the theoretical value of $\sqrt{2}$ may be because the steady state assumption is only approximately valid. Surface friction is absent in the model so this is not a contributing factor.

In summary, we determine the propagation speed according to Eq. 5, with $k = 1.1$ and take into account the change in low-level winds just ahead of the gust front. Table 6 shows 1) the surface pressure jump; 2) C_p determined from Eq. (5); 3) the wind change just ahead of the system from the basic state, Δu; 4) the predicted propagation speed relative to the surface, C^*; and 5) the simulated propagation speed. Figure 10 shows a plot of the simulated propagation speed versus the predicted. The agreement is quite reasonable considering some of the approximations that have been made. A certain amount of subjectivity is involved in estimating the pressure jump in some cases. However, overall, it seems that the predicted speeds using the surface pressure jump are more consistent with simulated speeds than those obtained based on the temperature perturbation in the cold pool.

It is possible to determine the separate contributions

TABLE 6. Determination of the predicted propagation speed C^*. Here ΔP is the estimated pressure jump, C_p the speed according to Eq. (5) and Δu the change in the winds in the lowest layer just ahead of the gust front.

Group and number	Experiment	ΔP	C_p	Δu	C^*	C_{sim}
	Control	0.8	9.2	−2.5	13.0	12.5
A1	Stronger jet	0.3	5.6	−1.1	8.0	7.9
A2	Weaker jet	0.4	6.5	−1.5	9.3	8.4
A4	Higher jet	0.2	4.6	−2.1	6.7	5.1
A5	Lower jet	0.5	7.3	−2.1	9.4	11.2
A6	Reduced shear aloft	0.7	8.6	−1.1	11.0	10.7
A7	Weak shear aloft	1.4	12.1	0.7	12.7	11.2
A8	Unidirectional shear	0.8	9.2	−0.1	10.6	10.7
A9	Stronger shear aloft	0.7	8.6	−1.0	10.9	11.2
A10	Stronger jet and weak shear aloft	0.2	4.6	−2.6	8.5	9.6
B1	Increased moisture	0.4	5.9	−2.1	9.3	11.8
B2	Decreased moisture	0.8	9.2	−3.3	13.8	12.9
B3	Increased buoyancy	0.9	9.7	−0.5	11.5	11.8
B4	Increased low level buoyancy	1.0	10.3	0.6	11.0	12.9
C1	Increased buoyancy and weak shear aloft	1.1	10.8	−0.4	12.5	12.3
C2	Increased buoyancy and unidirectional shear	1.3	11.7	−2.0	15.0	14.0
C3	Increased buoyancy, stronger jet, and weak shear sloft	1.3	11.7	−0.8	13.8	15.1
C4	Increased buoyancy and stronger jet	1.6	13.0	0.1	14.2	13.4
C5	Increased buoyancy and weaker jet	0.6	7.9	−0.7	9.9	9.0
C6	Increased low-level buoyancy, stronger jet, and weak shear aloft	1.5	12.6	2.3	11.6	13.4
C7	Weak shear aloft and increased moisture	0.7	8.6	−1.3	11.2	10.7
D2	No shear and less cooling	0.3	5.6	1.6	2.0	3.1
D3	Stronger jet and increased cooling	0.9	9.7	−2.0	13.0	13.4
D5	Stronger jet, weak shear sloft, and increased cooling	1.5	12.6	−2.9	16.8	15.1

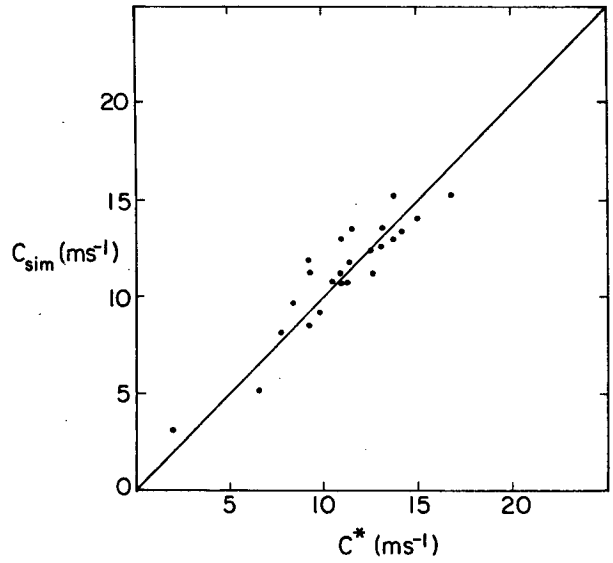

FIG. 10. Plot of simulated propagation speed (C_{sim}) between 3 and 4 h against predicted propagation speed (C^*).

to the surface pressure jump across the cold pool. Figure 11 schematically illustrates the relationship of the warming exterior to the cold pool and water loading, to the surface pressure jump. The hydrostatic contribution to the surface pressure jump due to warming ahead of the gust front, is generally less than that behind, but is still significant. Water loading is also usually less ahead of the gust front than behind. Water loading has the opposite effect of warming, tending to produce an increase in the pressure jump. In order to estimate these effects, the individual contributions to the surface pressure jump due to the cold pool, warming, and water loading are determined by integrating downwards the hydrostatic nondimensional pressure equation,

$$\frac{\partial \pi'_{\text{hyd}}}{\partial z} = \frac{g}{c_p \theta_{v0}} \left(\frac{\theta'_v}{\theta_{v0}} - q_w \right) \tag{6}$$

where θ'_v is the virtual potential temperature perturbation and q_w the total liquid and ice water mixing ratio. The nondimensional pressure is defined by

$$\pi = \left(\frac{p}{P} \right)^{R/c_p} \tag{7}$$

where P is the basic state surface pressure. The pressure perturbation at the top of the model is small and does not vary much between the positions of the surface low and high. To a good approximation, the surface pressure perturbation is given by

$$p'_{\text{sfc}} \approx \frac{c_p}{R} P \pi'_{\text{sfc}}. \tag{8}$$

This decomposition is performed for the six systems whose surface pressure fields are shown in Fig. 9. In order to reduce the nonhydrostatic component, quantities are averaged over a 5 km region, centered at the maxima and minima shown in these figures. Note that this averaging has the effect of reducing the magnitude of the pressure jump.

Results of these calculations are presented in Table 7. The first column shows the simulated pressure jump; the second, the contribution due to the cold pool; the third, the decrease in the surface pressure jump due to warming; the fourth, the increase in the pressure jump due to the effect of water loading; and the fifth, the nonhydrostatic contribution. This is calculated as the difference between the vertical nondimensional pressure gradient and the buoyancy terms (which of course are not generally in hydrostatic balance) integrated through the depth of the atmosphere. The sixth shows the ratio of the combined effect of warming and water loading to that of the cold pool. The pressure jump due to the cold pool is quite different in most cases from the observed pressure jump. The effect of warming on the surface pressure difference is typically as large as that due to the cold pool. This effect is negated to a certain extent by water loading. In these examples, the nonhydrostatic contribution tends to be smaller, though not insignificant. (In some instances it can be large.) For the control, C3, D2, and C6 the total effect of warming and water loading is about half that due to the cold pool. The result is to reduce ΔP by approximately one-half. However, in the case of A7, the effect of warming is completely negated by the effect of water loading. In the case of A8, the contribution due to the weight of condensation is twice as large as that due to warming. Hence, the pressure jump that actually occurs is larger than that due to the cold pool contribution. This is why the system moves faster than predicted by Eq. 4. Thus, the systems which are strongly tilted upshear (relative to the low-level winds) tend to move slower than predictions based only on the cold

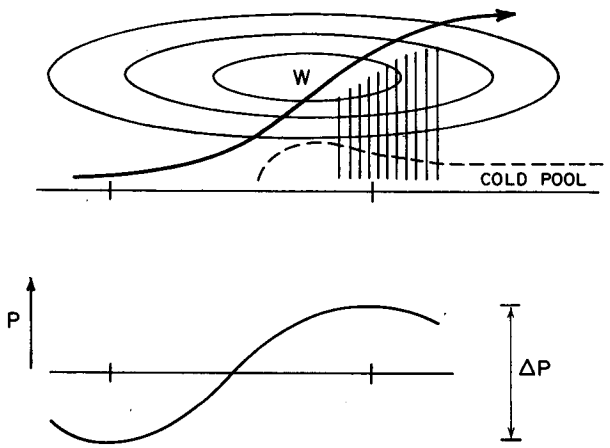

FIG. 11. Schematic showing relationship of warming and precipitation (vertical lines) to the surface pressure jump across the gust front.

TABLE 7. Contributions to the pressure jump. Here ΔP_{sim} is the observed pressure jump, ΔP_{cold} is the contribution due to the cold pool, ΔP_{warm} the decrease in the pressure jump due to warming, $\Delta P_{loading}$ the increase in the pressure jump due to water loading, and ΔP_{NONHYD} the nonhydrostatic contribution. The final column shows the ratio of the combined effect of warming and water loading to that of the cold pool.

Group and no.	Experiment	ΔP_{sim} (mb)	ΔP_{cold} (mb)	ΔP_{warm} (mb)	$\Delta P_{loading}$ (mb)	ΔP_{NONHYD} (mb)	$\frac{\Delta P_{warm} + \Delta P_{loading}}{\Delta P_{cold}}$
	Control	0.62	1.48	−0.89	0.17	−0.14	−0.49
A7	Weak shear aloft	1.4	1.17	−1.81	1.83	0.21	0.02
A8	Unidirectional shear aloft	0.4	0.19	−0.42	0.96	−0.33	2.8
C3	Increased buoyancy, stronger jet, and weak shear aloft	1.1	2.59	−2.59	1.2	−0.1	−0.54
C6	Increased low-level buoyancy, stronger jet, and weak shear aloft	1.22	3.15	−2.45	0.98	−0.46	−0.47
D2	No jet and less cooling	0.14	0.38	−0.2	0.01	−0.05	−0.5

density current model, the more vertically oriented systems move about the same speed, whereas the systems which tilt downshear tend to move faster. These effects are probably exaggerated in a two-dimensional model since updraft tilts are greater than observed. For the majority of squall lines the net effect of warming exterior to the cold pool and water loading on the surface pressure jump are likely to be small and the squall line speed close to that given by the density current model.

The surface pressure fields may be effected to a certain extent by the smallness of the domain, specifically by the MCR. The analysis above was performed at different times with a much larger domain (1000 km) and C3's environment. The results are consistent with those obtained above. At 1.5 h the system moves approximately 25% faster than predicted by the density current model, whereas at 3 h and longer (when the updraft has developed a significant upshear tilt), it moves 25% slower. The surface high accompanying the system, which is very narrow in these simulations at 3.5 h, is found to broaden significantly with time.

e. *Conditions for a vertical jet*

In this section, the vorticity balance that exists for experiment A7, which for much of the simulation has a vertically oriented updraft, is examined. Rotunno et al.'s (1988) optimum condition can be found by integrating the steady state vorticity equation from a point L ahead of the cold pool to a point R behind and up to a height d, where the inflow exits as a vertically oriented jet:

$$\int_0^d \int_L^R \frac{\partial}{\partial x} u\eta dx dz + \int_0^d \int_L^R \frac{\partial}{\partial z} w\eta dx dz = -\int_0^d \int_L^R \frac{\partial b}{\partial x} dx dz \quad (9)$$

where $\eta = \partial u/\partial z - \partial w/\partial x$ is the vorticity and b the buoyancy. The second term on the left-hand side is zero in the case of a vertically oriented jet. Recognizing that the vorticity ahead of the cold pool is $\sim \partial u/\partial z$, we obtain

$$\left(-\frac{u^2}{2}\right)_{L,d} + \left(\frac{u^2}{2}\right)_{L,0} + \int_0^d (u\eta)_R dz = -\int_0^d (b_R - b_L) dz. \quad (10)$$

They consider the situation where the vorticity at some distance behind the gust front is $\sim \partial u/\partial z$. Assuming that a stagnation point exists at the surface in the cold pool, and again using the condition that the inflow exits as a vertically oriented jet, at d, Eq. (10) becomes

$$\left(\frac{u^2}{2}\right)_{L,0} = -\int_0^d (b_R - b_L) dz. \quad (11)$$

If the buoyancy is confined to the cold pool and given by $g\theta'_v/\theta_{v0}$, then Eq. 1 is obtained. This relation implies a balance between the import of vorticity associated with the low-level environmental shear and the vorticity generation by the cold pool in the volume. Figures 12a and 12b show the wind vectors and vorticity fields, respectively, at 2 h, in the region of strong convection. There is negative vorticity on the left of the updraft and positive vorticity on the right, with the situation reversed for the low-level downdraft. Notice that there does not appear to be a position behind the gust front where $\partial w/\partial z$ is small and a stagnation point exists at the surface. Since the horizontal velocity is small through the center of the rear low-level downdraft, it may be that at this position the third term in Eq. (10) can be neglected and hence, Eq. (11) holds.

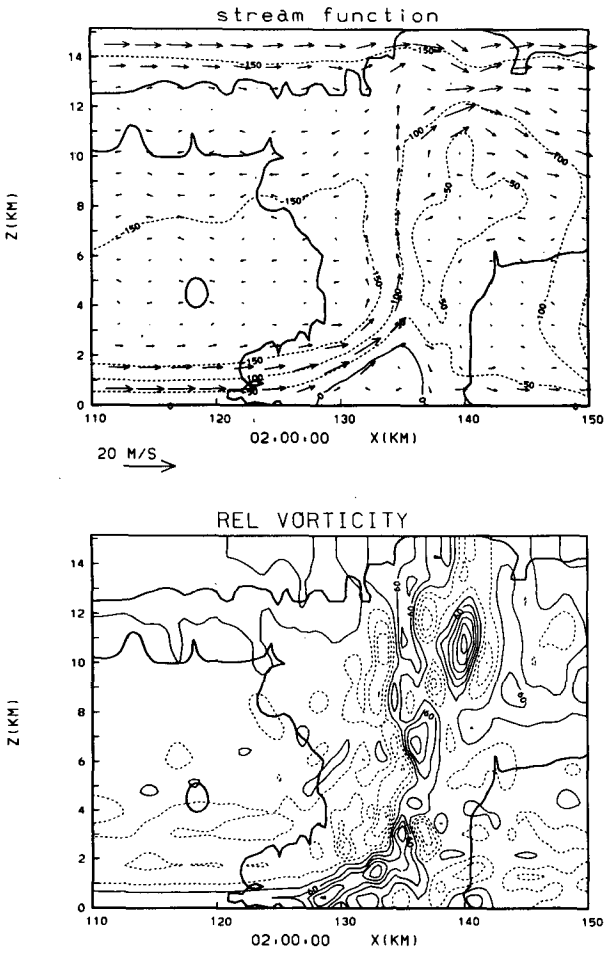

FIG. 12. Enlarged fields for A7 at 2 h: (a) Wind vectors and stream function. The contour interval is 500 $m^2 s^{-1}$ and the label scale is 10^{-1}. (b) Vorticity. The contour interval is 4×10^{-3} and the label scale is 10^4.

However, water loading and warming above the cold pool contribute significantly to the buoyancy if it is vertically integrated up to the height where the updraft becomes vertical. Because there are strong horizontal gradients in buoyancy at this position and the downdraft is not entirely steady, it is difficult to unequivocably determine the net effect of these other buoyancy contributions on the vorticity balance. Although the water loading and warming above the cold pool cancel one another to a certain extent, the net contribution to the buoyancy may not be insignificant. Hence, this situation is considerably different than envisioned by Rotunno et al. (1988). The conditions they use to derive the optimum condition is based on a quite different multicellular system, which forms in an environment having strong low-level shear and no shear aloft. The cells tilt downshear as they develop, leading to the detrimental effect of precipitation unloading into the inflow. The collapse of the cell produces a pronounced surge in the gust front which then initiates a new updraft. The new cell undergoes the same life cycle and the whole process exhibits very regular oscillatory behavior. For the unicell simulation it appears that the vorticity balance is not just an interaction of the low-level shear with the cold pool. The vorticity balance that occurs in the unicell may be a complex dynamic interaction. The pressure gradient responsible for decellerating the horizontal velocity of the inflow air is clearly related to water loading in the narrow precipitation shaft (see Fig. 3f). For a vertical updraft, water loading tends to counterbalance the negative contribution of warming to the hydrostatic component of the pressure field.

5. Discussion and conclusions

In the Introduction, two results concerning the effects of shear were stated. In the presence of a shallow cold pool, a certain optimum value of low-level shear exists, which leads to deep uplifting which can force convection (Rotunno et al. 1988). However, in the absence of vorticity sources and sinks, for instance above the cold pool, shear is detrimental to convection (Kuo 1963; Asai 1964). The results of this study are consistent with these findings. However, it is shown that the vorticity balance that occurs for a unicell system which has a vertical updraft is not purely one between the low-level shear and the cold pool. The effects of warming above the cold pool and water loading also need to be taken into account, and Eq. (11) only appears applicable at the center of the low-level downdraft. The structure of the systems are quite sensitive to the shear aloft. If the shear is strong and positive above the low-level jet, systems are multicellular and less intense. If the shear is weakly negative, then the updraft starts to tilt downshear relative to the low-level winds (for the standard buoyancy) and the detrimental effects of water loading and evaporation on the updraft lead to a less intense system. Most of the simulations undergo a transition from a vertically oriented updraft early on, to a more upshear tilted updraft as the cold pool becomes deeper and cooler. Clearly, the development of the cold pool is a complex issue. It is dependent on a variety of factors, such as the amount of buoyancy, the distribution of buoyancy in the vertical, the amount of midlevel moisture and the environmental wind structure. Experiments with increased buoyancy all produce deeper and cooler cold pools than simulations which have similar wind structures but the standard buoyancy. Presumably, this is because the precipitation rate and hence evaporation are increased. There is also a tendency for dry midlevel air to favor cold pool development. Environments with strong positive shear aloft produce tilted updrafts which encourage the formation of pronounced cold pools. The probable reason for this, suggested by Dudhia et al. 1987, is that a shallower updraft tilt causes precipitation to fall over a wider region. Consequently, parcels in the downdraft

experience evaporative cooling for a longer period, leading to enhanced cooling. Furthermore, the stronger the low-level jet, the deeper and cooler the cold pool. This is because simulated squall lines in environments having stronger jets are more intense and have a larger precipitation rate.

For the simulations which have increased buoyancy, none of the systems manage to maintain a vertically oriented updraft for very long. It is possible that by using a stronger low-level shear, with weak shear aloft, a more persistent vertically oriented updraft could be obtained. However, it is interesting that for D5, the case with standard buoyancy, a stronger jet, much less shear aloft and an increased initial cooling rate, the transition from a vertical to a tilted updraft occurs earlier than for A7 (weak shear aloft). Hence, the feedbacks that occur between the various processes involved are complex and not easy to predict.

Results of this study strongly suggest that the pressure jump that occurs across the gust front is a better determinant of propagation speed than the temperature perturbation in the cold pool. This agrees with the results of the study by Seitter (1986). It appears that for systems having vertically oriented or downshear tilted updrafts the effect of warming on reducing the pressure jump is negated or actually exceeded by the effect of water loading. As the updraft becomes more tilted due to a cooling and deepening of the cold pool, the squall line does not speed up as much as might be expected, since the effect of warming on reducing the pressure jump outweighs the effect of water loading. The reason this occurs may be because a vertically oriented updraft tends to suspend a large amount of condensate in the column of air above the gust front, which contributes significantly to the surface pressure rise. As the updraft tilts the amount of condensate in the column of air above the gust front is sharply reduced compared to the warming. For the majority of squall lines, these effects probably result in a fairly minor correction to the propagation speed predicted by the density current model. It has been suggested that propagation speed is related to that of forced linear internal gravity waves, as envisioned by wave-CISK theory (Raymond 1975, 1976). One may question the linear assumption for squall lines, since the shear is completely reversed from that of the environment in the region of strong convection. Furthermore, to parameterize convection, one has to hypothesize the interaction between the resolved scale and the smaller scale, which is extremely complex. Raymond (1983, 1984) includes the effects of downdrafts in a wave-CISK model. In addition to the usual propagating mode, an additional advecting mode is obtained. This mode grows rapidly in the early stages and then the disturbance divides into two parts which travel in opposite directions, which are identified as propagating modes. Only one of these traveling disturbances represents the real squall line. Raymond suggests that the reason for the spurious modes' existence is related to the insensitivity of the wave-CISK convective parameterization to midlevel ventilation. Another possible contributing factor is that the convective parameterization does not represent the interaction between low-level shear and a cold pool, which may occur on a scale which is not properly resolved. Although the realism of the convective parameterizations presently used in wave-CISK models is questionable, the degree to which a squall line can be thought of as a forced linear internal gravity wave remains an interesting idea. In particular, these simpler models suggest that the relation of warming aloft to the location of latent heat release is a complicated problem in gravity wave dynamics. This aspect warrants further study.

Experiments in which the midlevel moisture is altered suggest that dry midlevel air is not particularly favorable for tropical squall lines. Simulations in which the distribution of buoyancy is changed so that it is large at low levels and reduced aloft do not produce significantly stronger maximum updraft speeds (although the systems are more intense in some respects). This is probably because this environment is conducive to forming a cooler and deeper cold pool which tends to produce very tilted updrafts for the values of low-level shear used in this study.

In this paper we have investigated the sensitivity of tropical squall lines to environmental profiles. There is clearly a need for sensitivity studies to physical parameterizations. In particular, the importance of ice processes needs to be clarified and improvements made in the way they are parameterized in the model. There is also a need for further investigations of the mechanisms leading to the formation of squall lines. Initialization by a large deformation within a surrounding horizontally homogeneous environment is plainly artificial. Another limitation of this modeling study is the two dimensionality. Simulated updrafts appear to have shallower slopes than observed. Subsidence warming is most likely exaggerated, as are gravity waves. The cellular nature of convection may be of a somewhat different character in three dimensions than in two. New cells may be formed at the intersections of downdraft outflows from older cells, a process not simulated in two dimensions. In order to clarify these differences, a detailed comparison of a two-dimensional and a three-dimensional simulation of a squall line has been carried out and will be reported in a forthcoming paper.

Acknowledgments. The authors thank Drs. Gregory Tripoli and James Toth for their very helpful comments. Dr. Richard Rotunno and his colleagues were kind enough to make available the results of their research. Thanks to Gail Cordova for preparing this manuscript.

Acknowledgment is made to the National Center for Atmospheric Research, which is sponsored by the National Science Foundation, for the computing time

used in this research. This research has been supported by the Division of the Atmospheric Sciences, National Science Foundation under Grants ATM-8507961 and ATM-8206808.

REFERENCES

Asai, T., 1964: Cumulus convection in the atmosphere with vertical wind shear: Numerical experiment. *J. Meteor. Soc. Japan,* **42,** 245–259.

Benjamin, J. B., 1968: Gravity current and related phenomena. *J. Fluid Mech.,* **31,** 209–248.

Dudhia, J., M. W. Moncrieff and D. W. K. So, 1987: The two-dimensional dynamics of west African squall lines. *Quart. J. Roy. Meteor. Soc.,* **113,** 121–146.

Hane, C., 1973: The squall line thunderstorm: Numerical experimentation. *J. Atmos. Sci.,* **30,** 1672–1690.

Klemp, J. B., and D. K. Lilly, 1978: Numerical simulation of hydrostatic mountain waves. *J. Atmos. Sci.,* **35,** 78–107.

Kuo, H. L., 1963: Perturbations of plane couette flow in stratified fluid and origin of cloud streets. *Phys. Fluids,* **6,** 195–211.

LeMone, M. A., 1983: Momentum flux by a line of cumulonimbus. *J. Atmos. Sci.,* **40,** 1815–1834.

Lilly, D. K., 1985: The structure, energetics and propagation of rotating storms. Part I: Energy exchange with the mean flow. *J. Atmos. Sci.,* **43,** 113–125.

Lin, Y.-L., 1987: Response of a stably stratified shear flow to diabatic heating. *J. Atmos. Sci.,* **44,** 1375–1393.

Lindzen, R. S., and K. K. Tung, 1976: Banded convective activity and gravity waves. *Mon. Wea. Rev.,* **104,** 1602–1617.

Moncrieff, M. W., and M. J. Miller, 1976: The dynamics and simulation of tropical cumulonimbus and squall lines. *Quart. J. Roy. Meteor. Soc.,* **102,** 373–394.

Nicholls, M. E., 1987: A comparison of the results of a two dimensional numerical simulation of a tropical squall line with observations. *Mon. Wea. Rev.,* **115,** 3055–3077.

Raymond, D. J., 1975a: A model for predicting the movement of continuously propagating convective storms. *J. Atmos. Sci.,* **32,** 1308–1317.

——, 1975b: Application of a generalized "impedance relationship" to mesoscale convergence lines. *J. Atmos. Sci.,* **32,** 1894–1897.

——, 1976: Wave-CISK and convective mesosystems. *J. Atmos. Sci.,* **33,** 2392–2398.

——, 1983: Wave-CISK in mass flux form. *J. Atmos. Sci.,* **40,** 2561–2572.

——, 1984: A wave-CISK model of squall lines. *J. Atmos. Sci.,* **41,** 1946–1958.

Rotunno, R., and J. B. Klemp, 1982: The influence of the shear-induced pressure gradient on thunderstorm motion. *Mon. Wea. Rev.,* **110,** 136–151.

——, —— and M. L. Weisman, 1988: A theory for strong, long-lived squall lines. *J. Atmos. Sci.,* **45,** 463–485.

Seitter, K. L., 1986: A numerical study of atmospheric density current motion including the effects of condensation. *J. Atmos. Sci.,* **43,** 3068–3076.

Soong, S.-T., and W.-K. Tao, 1984: A numerical study of the vertical transport of momentum in a tropical rainband. *J. Atmos. Sci.,* **41,** 1049–1061.

Szoke, E. J., and E. J. Zipser, 1986: A radar study of convective cells in mesoscale systems in GATE. Part II: Life cycles of convective cells. *J. Atmos. Sci.,* **43**(2), 199–218.

Thorpe, A. J., M. J. Miller and M. W. Moncrieff, 1982: Two-dimensional convection in nonconstant shear: A model of mid-latitude squall lines. *Quart. J. Roy. Meteor. Soc.,* **108,** 739–762.

Tripoli, G. J., 1986: A numerical investigation of an orogenic mesoscale convective system. Ph.D. dissertation, Colorado State University.

——, and W. R. Cotton, 1982: The Colorado State University three-dimensional cloud/mesoscale model—1982. Part 1: General theoretical framework and sensitivity experiments. *J. de Rech. Atmos.,* **16,** 185–220.

Wakimoto, R. M., 1982: The life cycle of thunderstorm gust fronts as viewed with doppler radar and rawinsonde data. *Mon. Wea. Rev.,* **110,** 1050–1082.

Zipser, E. J., R. J. Meitin and M. A. LeMone, 1981: Mesoscale motion field associated with a slowly moving GATE convective band. *J. Atmos. Sci.,* **38,** 1725–1750.